2014

Chelation and Stereodynamic Equilibria in Neutral Hypercoordinate Organosilicon Complexes of 1-Hydroxy-2-pyridinone

Bradley M. Kraft
St. John Fisher College, bkraft@sjfc.edu

William W. Brennessel
University of Rochester

Publication Information

Kraft, Bradley M. and Brennessel, William W. (2014). "Chelation and Stereodynamic Equilibria in Neutral Hypercoordinate Organosilicon Complexes of 1-Hydroxy-2-pyridinone." *Organometallics* 33.1, 157-171.

Chelation and Stereodynamic Equilibria in Neutral Hypercoordinate Organosilicon Complexes of 1-Hydroxy-2-pyridinone

Abstract

A series of neutral organosilicon compounds, R3Si(OPO) [R = Me (1), Et (2), Ph (3)], cis-R2Si(OPO)2 [R = Me (4), Et (5), iPr (6), tBu (7), Ph (9)], (CH2)3Si(OPO)2 (8), and cis-R2Si(OPO)Cl [R = Me (10), Et (11)] (OPO = 1-oxo-2-pyridinone) have been prepared and fully characterized. X-ray crystallographic analyses show 1 to be tetracoordinate, 3, 7, and 10 to be pentacoordinate, and 4, 5, 6, 8, and 9 to be hexacoordinate. In the hexacoordinate structures, a mixture of diastereomers is observed in the form of C/N site disorder in each OPO ligand. Variable-temperature 13C and 29Si NMR studies indicate reversible Si←OC bond dissociation occurring in all pentacoordinate and hexacoordinate complexes to a varying degree with greater tendency toward dissociation in hydrogen-bonding donor solvents. Significant weakening of the dative Si←OC bond in 3 is observed in the co-crystallized adduct solvate, 3·Ph3SiOH·½C5H12, providing structural evidence for the decrease in coordination number of the OPO ligand by hydrogen-bonding donors. In the hexacoordinate complexes, increasing steric bulk of ancillary ligands also was found to promote dissociation. 1H and 13C VT-NMR studies of 4, 6, 8, and 9 indicate stereoisomerization equilibria concurrent with Si←OC bond dissociation proposed to occur through trigonal bipyramidal intermediates. 1

Disciplines

Chemistry

Chelation and Stereodynamic Equilibria in Neutral Hypercoordinate Organosilicon Complexes of 1-Hydroxy-2-Pyridinone

Bradley M. Kraft*[†] and William W. Brennessel[‡]

[†] *Department of Chemistry, St. John Fisher College, Rochester, NY 14618, USA*
[‡] *Department of Chemistry, University of Rochester, Rochester, NY 14627, USA*

For Table of Contents Only:

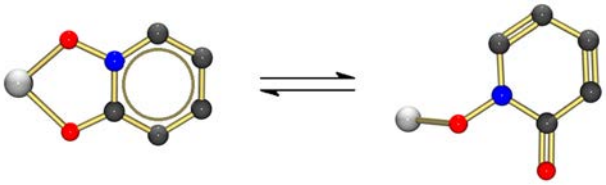

Abstract

A series of neutral organosilicon compounds, $R_3Si(OPO)$ [R = Me (**1**), Et (**2**), Ph (**3**)], *cis*-$R_2Si(OPO)_2$ [R = Me (**4**), Et **(5**), ^{i}Pr (**6**), ^{t}Bu (**7**), Ph (**9**)], $(CH_2)_3Si(OPO)_2$ (**8**), and *cis*-$R_2Si(OPO)Cl$ [R = Me (**10**), Et (**11**)] (OPO = 1-oxo-2-pyridinone) have been prepared and fully characterized. X-ray crystallographic analyses show **1** to be tetracoordinate, **3**, **7**, and **10** to be pentacoordinate, and **4**, **5**, **6**, **8**, and **9** to be hexacoordinate. In the hexacoordinate structures, a mixture of diastereomers is observed in the form of C/N site disorder in each OPO ligand. Variable-temperature ^{13}C and ^{29}Si NMR studies indicate reversible Si←OC bond dissociation occurring in all pentacoordinate and hexacoordinate complexes to a varying degree with greater tendency toward dissociation in hydrogen-bonding donor solvents. Significant weakening of the dative Si←OC bond in **3** is observed in the co-crystallized adduct solvate, **3**·Ph_3SiOH·½C_5H_{12}, providing structural evidence for the decrease in coordination number of the OPO ligand by hydrogen-bonding donors. In the hexacoordinate complexes, increasing steric bulk of ancillary ligands also was found to promote dissociation. ^{1}H and ^{13}C VT-NMR studies of **4**, **6**, **8**, and **9** indicate stereoisomerization equilibria concurrent with Si←OC bond dissociation proposed to occur through trigonal bipyramidal intermediates.

Introduction

Silicon compounds with expanded coordination spheres, known as 'hypercoordinate' complexes, have been studied for a long time.[1] One class of these complexes possesses chelate ring(s) with hemilabile[2] ligand(s) which bear one inert and one labile heteroatom donor. Examples of neutral complexes of this type exhibiting dynamic Si←N or Si←O dative bond rupture include those based on *N*,*N*-dimethylbenzylamine,[3] tropolone,[4] acetylacetone,[5] quinolone,[6] salicylaldimine,[7] hydrazide,[8] acetamide,[9] prolinamide,[10] and glutarimide[11] ligands, among many others. These complexes are fundamentally interesting with respect to dynamic changes in their coordination mode, with their dative interactions often strongly being influenced by solvent, temperature, and substituent effects.

In view of the dynamic behavior observed in many hypercoordinate neutral silicon complexes, the study of complexes bearing the 1-oxo-2-pyridinone (OPO) ligand was particularly attractive. Although the OPO ligand is monovalent, it is only known to form chelate complexes similar to the isoelectronic and structurally-equivalent divalent catecholate ligand.[12] From either of its 2-pyridinone or *N*-oxide tautomeric forms, the OPO ligand chelates formally through an oxyanion and a dative oxo linkage (Figure 1). In one of its resonance structures having π-electron delocalization, the ligand may be viewed as a 'coordinated countercation' which may strengthen the chelate resulting from greater ionic character in the bonding. A similar situation occurs in the chelation of tropolone.[4]

Figure 1. Resonance forms of chelated OPO complexes

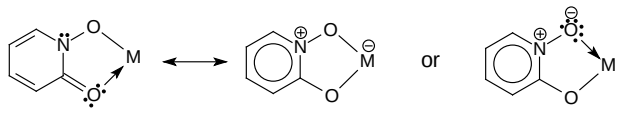

The chelate effect of the OPO ligand and related derivatives plays an important role in their effectiveness as sequestering agents,[13] and in the stability of their complexes in various medical applications.[12a,14] To the best of our knowledge, dissociative equilibria involving the OPO ligand have not been reported for any metal or metalloid complex and there are also no known reports of an isolated metal complex bearing a monodentate OPO ligand. $Co(OPO)_3$ and

$NbO(OPO)_3$ complexes are known for which stereodynamic processes were evident, but evidence for bond rupture was not observed.[13a,15]

Hexacoordinate cationic silicon complexes of the form $[Si(OPO)_3]^+X^-$ (X = Cl, $FeCl_4$, ½$SnCl_6$) were first prepared by Weiss and Harvey[16] and later characterized spectroscopically and structurally by Tacke, et al.[17] Beyond this homoleptic variety, only a handful of organosilicon complexes bearing the OPO ligand have been reported.[18] Studies involving organosilicon complexes were undertaken here to examine their potential dynamic nature. The use of electron-donating carbon-based ancillary ligands has proven appropriate for promoting weak Si←OC dative bonding interactions and has led to the discovery of the first well-defined examples of the hemilabile nature of the rigid OPO ligand.

Results and Discussion

$R_3Si(OPO)$ Complexes. Monosubstituted complexes, $R_3Si(OPO)$ [R = Me (**1**), Et (**2**), Ph (**3**)], were synthesized in quantitative yield in THF at room temperature with the assistance of triethylamine (eq 1). Filtration of the NEt_3HCl salt and removal of the solvent under vacuum gave highly moisture-sensitive compounds **1** and **3** as colorless solids and **2** as an oil. The ^{29}Si NMR chemical shifts of **1** and **2** appear at +35.2 and +35.7 ppm, respectively, supporting tetracoordinate solution structures.[19] For **3**, a higher field ^{29}Si NMR resonance appearing at −10.8 ppm also indicates a tetracoordinate structure.[20] Variable-temperature (VT) NMR studies of **3** revealed a dynamic equilibrium between 5- and 4-coordinate states (vide infra).

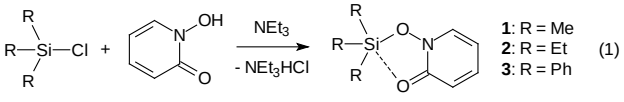

The crystal structure of **1** shows an effectively monodentate OPO ligand (Figure 2). Selected bond distances and angles are shown in Table 1. The coordination environment around silicon is approximately tetrahedral [∠O–Si–C's and ∠C–Si–C's range from 102.4–113.2°] with a covalent bond formed with the hydroxylamine oxygen of the ligand. The very weak Lewis acidity of the Me_3Si group is emphasized by the long Si1–O2 distance of 3.4945(15) Å which is just under the sum of the Si and O van der Waals radii of 3.62 Å.[21] The C=O bond distance

[1.230(2) Å] is shorter than the C=O bond in the free ligand (1.260 Å) which is consistent with the relief of the intermolecular H-bonding that exists in the neutral ligand[22] and compares with the C=O distances in known cyclohexyl- and benzyl-substituted OPO derivatives (1.233 Å and 1.223 Å, respectively).[23] The N–O distance is slightly longer than in the neutral ligand (1.377 Å). The presence of alternating long/short bonds in the pyridine ring indicates a localized system of π-bonding with the C1–C2 and C3–C4 bond distances (Avg. 1.423 Å) longer than the C2–C3 and C4–C5 bond distances (avg. 1.357 Å), similar to the sequence of bond lengths in the free ligand[22] and benzyl derivative.[23b] The structures of **1** and **2** are therefore similar to their carbon analogs favoring predominantly 2-pyridinone structures over their zwitterionic *N*-oxide tautomers.[22,24]

Figure 2. Crystal structure of **1** showing displacement ellipsoids at the 50% probability level.

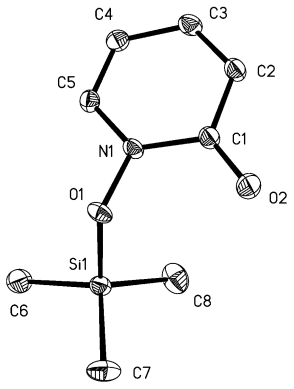

Table 1. Selected bond distances (Å) and angles (°) for monosubstituted complexes **1**, **3**, **3**·Ph_3SiOH·½C_5H_{12}, and **10**.

1		**3**		**3·Ph_3SiOH·½C_5H_{12}**		**10**	
Si1-O1	1.7120(14)	Si1-O1	1.7281(12)	Si1-O1	1.6960(19)	Si1-O1	1.7553(7)
Si1-O2	3.4945(15)	Si1-O2	2.1851(12)	Si1-O2	3.366(2)	Si1-O2	1.8833(8)
Si1-C6	1.8524(18)	Si1-C6	1.9071(15)	Si1-C6	1.851(3)	Si1-Cl1	2.2498(4)
Si1-C7	1.841(2)	Si1-C12	1.8679(15)	Si1-C12	1.862(3)	Si1-C6	1.8572(12)
Si1-C8	1.846(2)	Si1-C18	1.8771(16)	Si1-C18	1.847(3)	Si1-C7	1.8518(10)
N1-O1	1.3814(18)	N1-O1	1.3701(16)	N1-O1	1.388(3)	N1-O1	1.3694(10)
C1-O2	1.230(2)	C1-O2	1.2636(19)	C1-O2	1.247(3)	C1-O2	1.2930(11)
Si1-O1-N1	117.63(10)	Si1-O1-N1	120.62(9)	Si1-O1-N1	116.15(14)	Si1-O1-N1	114.21(5)
C6-Si1-O1	107.74(8)	O2-Si1-O1	78.73(5)	C6-Si1-O1	102.66(10)	O2-Si1-O1	84.09(3)
C7-Si1-O1	102.41(8)	O2-Si1-C12	82.71(5)	C12-Si1-O1	107.17(10)	O2-Si1-C6	93.02(5)
C8-Si1-O1	110.25(9)	O2-Si1-C18	83.77(6)	C18-Si1-O1	110.88(10)	O2-Si1-C7	90.34(4)
		O2-Si1-C6	169.23(6)			O2-Si1-Cl1	167.52(3)
		C6-Si1-O1	90.85(6)			Cl1-Si1-O1	83.47(2)
		C6-Si1-C12	104.17(7)			Cl1-Si1-C6	93.85(4)
		C6-Si1-C18	100.04(7)			Cl1-Si1-C7	95.06(4)
		C12-Si1-O1	113.27(6)			C7-Si1-O1	120.61(5)
		C12-Si1-C18	116.89(7)			C7-Si1-C6	120.83(6)
		C18-Si1-O1	123.71(7)			C6-Si1-O1	118.50(5)

The weak dative Si←OC interaction observed in **1** is apparently weaker in **2** at room temperature. Collected as KBr pellets, strong IR C=O stretching bands at 1649 cm^{-1} and 1653 cm^{-1} were observed for **1** and **2**, respectively. Both C=O stretches appear at higher wavenumbers than that observed in the free ligand (1640 cm^{-1}) from the relief of intermolecular H-bonding in the neutral ligand. The C=O stretching frequency in $^tBu_2Si(OPO)_2$ (**7**) described later, which possesses a monodentate OPO ligand in the solid state, also has a CO band at 1653 cm^{-1}, which suggests the absence of an Si←OC interaction in **2**. The apparent weaker Si←OC interaction in **2** vs. **1** might be from increased sterics or from increased entropic effects due to differences in their physical states, with **2** being a liquid and **1** being a solid at room temperature.

The solid-state structure of **3** reveals a distorted *cis*-trigonal bipyramidal coordination sphere with a chelated OPO ligand (Figure 3). Deviation from a regular TBP polyhedron is seen in the apical O–Si–C angle of 169.23(6)° and in the sum of the angles in the equatorial plane amounting to 353.87(12)°. A shorter/covalent Si–ON bond is formed in an equatorial position and a longer/dative Si←OC interaction is formed in an axial position. The bidentate OPO ligand forms a bite angle of 78.73(5)° and thus minimizes chelate ring strain by spanning axial and equatorial sites. The C=O bond is elongated in comparison to those in the non-chelated OPO

ligands in **1** and **7** (Table 2). The O_2Si unit and the planar OPO ligand form a dihedral angle of 6.66(5)°. Similar core structures are seen in a chelated $(C_6F_5)_3Si$ salicylaldimine complex[25] and the related triphenylpyrithione Sn derivative.[26] In the Sn pyrithione derivative, the hydroxylamine oxygen occupies an axial position vs. an equatorial position.

Figure 3. Crystal structure of **3** at the 50% probability level.

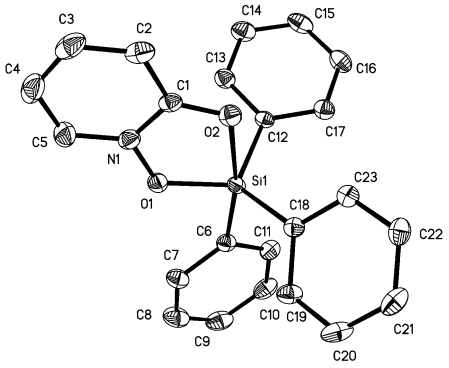

$R_2Si(OPO)_2$ Complexes. Disubstituted complexes, $R_2Si(OPO)_2$ [R = Me (**4**), Et (**5**), ^{i}Pr (**6**), ^{t}Bu (**7**)] and $(CH_2)_3Si(OPO)_2$ (**8**), were synthesized in quantitative yield by the same methodology as for the monosubstituted complexes (eq 2). The reactions proceed at room temperature except for the synthesis of **7** which required heating at 70 °C for several hours.

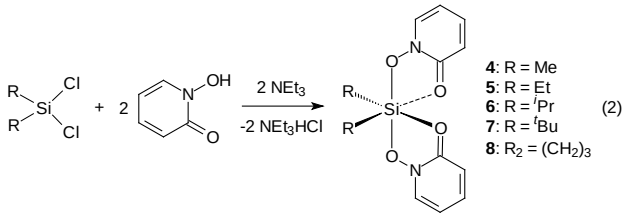

(2)

The synthesis of $Ph_2Si(OPO)_2$ (**9**) by the same method was not possible due to its insolubility which prevented its separation from the NEt_3HCl byproduct. By transsilylation, reaction of Ph_2SiCl_2 with 2 equiv. of **1** in $CHCl_3$ under dilute conditions produced **9** in about 50% yield upon crystallization from solution over several days (eq 3).

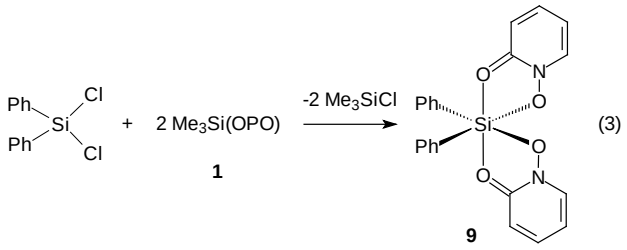

The ^{29}Si NMR spectra of **4**, **5**, **6**, **8**, and **9** in $CDCl_3$ at room temperature each exhibit a single peak at –106.4, –103.3, –101.1, –117.6, and –133.7 (DMSO-d_6), respectively, all of which suggest hexacoordinate solution structures.[27] The ^{29}Si NMR spectrum of **7**, however, exhibits a peak at –54.3 ppm which is consistent with a pentacoordinate structure.[28] For complexes **4**, **5**, **6**, **7**, and **8**, the ^{1}H and ^{13}C NMR spectra exhibited chemical-shift equivalent OPO ligand resonances at room temperature, whereas in **9** the spectra were complicated by severe broadening. VT-NMR studies indicate OPO chelation and stereoisomerism equilibria in all of these complexes (vide infra).

The X-ray structures of **4**, **5**, **6**, **8**, and **9** are shown in Figures 4, 5, 6, 7, and 8. Selected bond distances and angles are shown in Table 2. All five structures are similar. In **4**, **5**, **6**, and **9**, distorted octahedral geometries are exhibited with the maximum deviation from ideal 90° angles ranging from 9.08-11.41° and O–Si–O bite angles of about 82°. In **8**, the maximum deviation from 90° occurs in the metallacycle, forming a narrow C–Si–C angle of 77.12(4)° and also larger O–Si–O bite angles. Carbon-based groups are arranged in *cis*-isomeric form similar to the related Ph_2Si(tropolonato)$_2$ and $Me_2Si(thd)_2$ (thd = 2,2,6,6-tetramethyl-3,5-heptanedionato) complexes.[4a,29] The planar OPO ligands and the O_2Si chelate rings form dihedral angles of 1.78(4)° and 12.47(3)° in **4**, 7.10(4)° and 8.73(3)° in **5**, 2.68(3)° and 5.44(4)° in **6**, 3.22(2)° and 4.42(4)° in **8**, and 21.51(9)° in **9**. The greater dissimilarity between the two dihedral angles in **4** compared with the differences in **5**, **6**, or in **9** is possibly due to the intermolecular π-stacking of the pyridine ring that forms the larger of the dihedral angles, although π-stacking also occurs with one of the rings in **8** for which the angles are similar. In **9**, a very weak intermolecular CH…π interaction is present between the deviant OPO ligand and a phenyl ligand, but otherwise, there are no unusual interactions in the structure to explain the unusually large deviation from coplanarity. For comparison, the corresponding dihedral angles in the related Ph_2Si(tropolonato)$_2$ complex are much smaller (2.04° and 0.42°), and only one other OPO metal

chelate complex has been reported with this angle exceeding 20°.[12f] The Si–C bond lengths increase slightly in the order **4** < **5** < **6**.

Table 2. Selected bond distances (Å) and angles (°) for disubstituted complexes **4**, **5**, **6**, **8**, and **9**.[a]

	4	**5**	**6**	**8**	**9**[b]
Si1-O1	1.8315(6)	1.8347(6)	1.8313(6)	1.8324(6)	1.9175(14)
Si1-O3	1.8321(6)	1.8355(6)	1.8364(6)	1.8307(6)	-
Si1-O2	1.9118(7)	1.9148(6)	1.9302(7)	1.9016(6)	1.8157(13)
Si1-O4	1.9406(7)	1.9381(6)	1.9188(6)	1.8810(6)	-
Si1-C	1.9058(9)	1.9070(8)	1.9341(8)	1.9129(8)	1.920(2)
Si1-C	1.9007(9)	1.9146(8)	1.9327(8)	1.9144(8)	-
C-Si1-C	98.95(4)	100.14(4)	98.11(4)	77.12(4)	98.39(12)
O1-Si1-O2	82.78(3)	82.88(2)	82.54(2)	83.20(2)	82.47(6)
O3-Si1-O4	82.51(3)	82.30(3)	82.36(3)	83.96(3)	-

[a] The values of the C–N, N–O, and C–O bond lengths cannot be represented accurately because of OPO ligand disorder in all of these complexes.

[b] The molecule lies along a crystallographic two-fold axis that includes atom Si1; thus one half is unique.

A mixture of diastereomers is indicated in each crystal structure of **4**, **5**, **6**, **8**, and **9** by varying levels of disorder of the oxygen-coordinated N and C atoms in each bidentate ligand.[30] For these $(AB)_2MX_2$ systems with *cis* X groups, only 3 diastereomers are possible, specifically those with O(N)-*trans*-O(N), O(N)-*trans*-O(C), and O(C)-*trans*-O(C) arrangements. The N1/C1 and N2/C6 atom statistical disorder ratios of 66:34 and 79:21 in **4**, 81:19 and 82:18 in **5**, 84:16 and 59:41 in **6**, and 59:41 and 77:23 in **8** point generally to a higher probability of O(N)-*trans*-O(N) arrangements. Thus, coupled with the pairs of similar but longer Si–OC bonds (both ~1.9 Å) and similar but shorter Si–ON bonds (both ~ 1.8 Å), the formal assignment of longer dative Si←OC bonds and shorter covalent Si–ON bonds is suggested, as seen in non-disordered structures **1**, **3**, **7**, and **10**. Overall, in comparison with **4**, **5**, and **6**, slightly shorter pairs of Si–O bond lengths in **8** and even more so in **9** are observed (Table 2). These differences are consistent with the greater Lewis acidity of silacyclobutane complexes[31] and the more electron-withdrawing quality of phenyl vs. alkyl which is expected to strengthen the Si–O bonds.

The average C/N disorder ratio (60:40 for both C1/N1 and C1A/N1A due to symmetry) in **9** indicates a higher probability of the O(C)-*trans*-O(C) arrangement than in the other $R_2Si(OPO)_2$ complexes. This was puzzling in light of the fact that the positions of the long and short pairs of Si–O bonds as in **4**, **5**, **6**, and **8** are the same as in **9**. This observation negates the basic assumption that Si–OC bonds are always formally dative and thus weaker than Si–ON bonds. The cause of the reversal in relative Si–ON and Si–OC bond lengths appears to stem from the *trans* influence of the alkyl/phenyl groups. In structures **4**, **5**, **6**, and **9**, Si–O bonds *trans* to alkyl/phenyl groups are always on average ~0.1 Å longer than those *cis* and thus independent of the disorder ratios. This suggests that the *trans* influence gives rise to all possibilities of dative and covalent Si–ON and Si–OC bonds in all of the structures to a varying degree. Further support for the greater *trans* effect by alkyl/phenyl groups is given by the identical Si–O bond lengths observed in the C/N-disordered $[Si(OPO)_3]^+$ complex (*fac*:*mer* = 1:3) having no alkyl groups,[17] and by structural comparison with the related *cis*-$Ph_2Si(tropolonato)_2$ complex.[4a] Even with the symmetric tropolonato ligand where no ligand-centered influence on the Si–O bond lengths exists, phenyl groups are observed to be *trans* to the longer pair of Si–O bonds, and also happen to be ~0.1 Å longer than those *cis*. Evidence presented later for the rapid interconversion of these $R_2Si(OPO)_2$ diastereomers in solution suggests that the energy differences between these isomers are small.

Figure 4. Crystal structure of **4** at the 50% probability level.

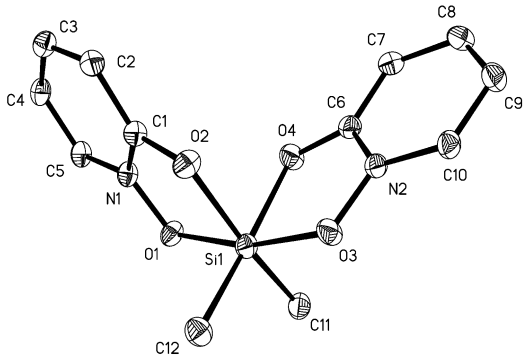

Figure 5. Crystal structure of **5** at the 50% probability level.

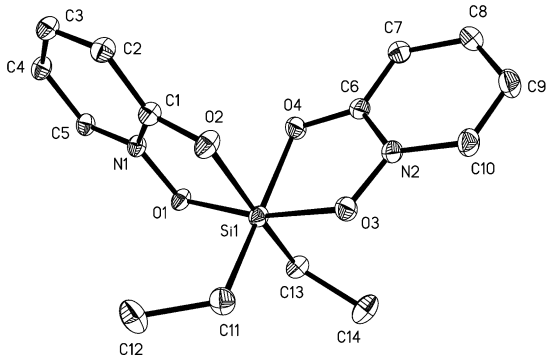

Figure 6. Crystal structure of **6** at the 50% probability level.

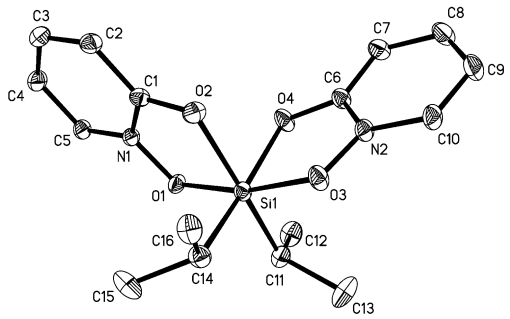

Figure 7. Crystal structure of **8** at the 50% probability level.

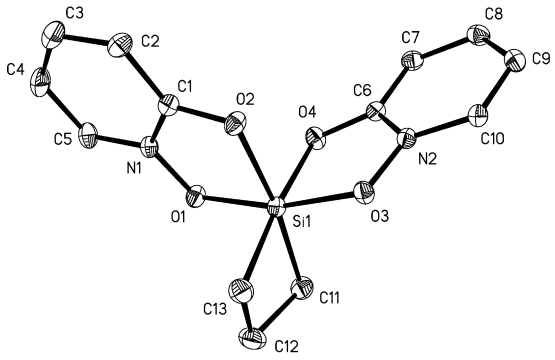

Figure 8. Crystal structure of **9** at the 50% probability level.

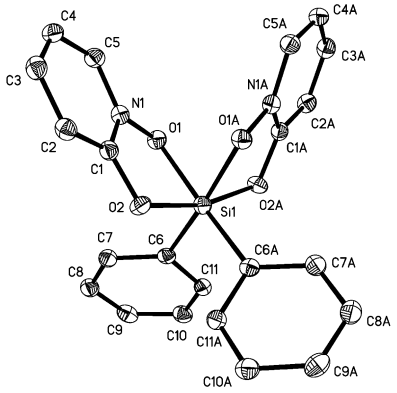

The solid-state structure of **7** reveals a 5-coordinate distorted TBP structure with one bidentate OPO ligand and one monodentate OPO ligand (Figure 9). Deviation from a regular TBP polyhedron is seen in the apical O–Si–O angle of 165.37(5)° and in the sum of the angles in the equatorial plane amounting to 359.55(11)°. The bidentate OPO ligand forms a shorter covalent Si—ON bond in an equatorial position and a longer Si←OC dative bond in an axial position to form a bite angle of 81.75(5)°. The occupation of the hydroxylamine oxygen in the equatorial plane is the same as in other TBP structures **3** and **10**. The second OPO ligand is characterized as monodentate by the long Si–O4 distance [4.1343(12) Å] which is well outside the sum of the Si and O van der Waals radii.[21] Because there are no unusual intermolecular contacts in the

crystal structure of **7** to suggest lattice stabilization of the monodentate OPO ligand against coordination, steric bulk is likely responsible for the monodentate coordination mode. The bulky ^{t}Bu groups occupy equatorial positions similar to the arrangement in a number of pentacoordinate TBP Sn complexes.[32]

Figure 9. Crystal structure of **7** at the 50% probability level. Selected bond distances (Å) and angles (°): Si–O1, 1.7742(11); Si–O3, 1.7822(11); Si–O2, 1.9273(11); Si–O4, 4.1343(12); C1–O2, 1.2812(18); C6–O4, 1.2411(18); N1–O1, 1.3692(15); N2–O3, 1.3724(15); C1–N1, 1.3491(19); C6–N2, 1.3994(19); Si–C11, 1.9069(16); Si–C15, 1.9191(16); C11–Si–C15, 122.40(7); O1–Si–C15, 121.97(6); C11–Si–O1, 115.18(6); O3–Si–C11, 89.79(6); O2–Si–C11, 93.17(6).

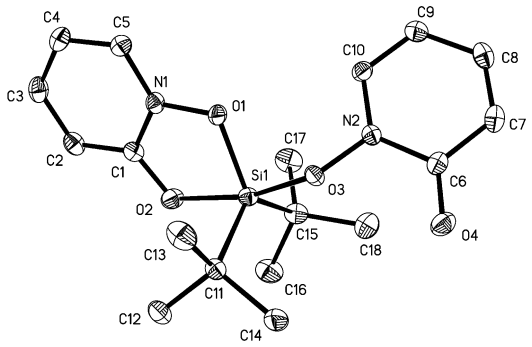

R_2Si(OPO)Cl Complexes. Reaction of Me_2SiCl_2 or Et_2SiCl_2 with 1 equiv. of HOPO and NEt_3 in THF at room temperature produced the monosubstitution products, Me_2Si(OPO)Cl (**10**) and Et_2Si(OPO)Cl (**11**), respectively (eq 4). The solution ^{29}Si NMR spectra of **10** and **11** show single peaks at –38.0 and –35.1 ppm, respectively, consistent with pentacoordinate structures.

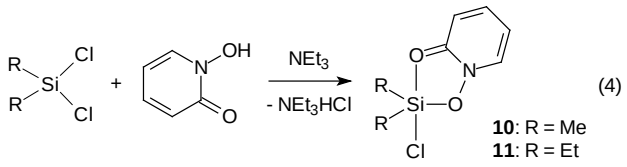

(4)

The X-ray structure of **10** reveals a distorted TBP coordination sphere (Figure 10). Deviation from a regular TBP polyhedron is seen in the apical O–Si–Cl angle of 167.52(3)° and in the sum

of the angles in the equatorial plane amounting to 359.94(9)°. The bidentate OPO ligand forms a shorter covalent Si–ON bond in an equatorial position and a longer dative Si←OC bond in an axial position and forms a bite angle of 84.09(3)°. The O_2Si unit and the OPO ligand are nearly coplanar [dihedral angle = 3.13(6)°]. The observed apicophilicity of the chloride ligand is similar to that seen in other pentacoordinated neutral chlorosilanes.[33]

Figure 10. Crystal structure of **10** at the 50% probability level.

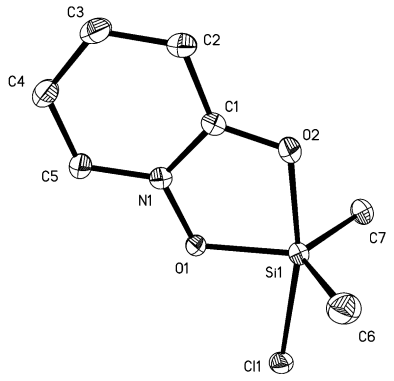

Efforts to obtain analytically pure samples of **10** and **11** were unsuccessful due to ligand redistribution equilibria (eq 5). Drying samples of **10** or **11** under vacuum resulted in ~5% wt. contamination by **4** and ~ 12% wt. contamination by **5**, respectively (see Supporting Information). The mass lost by the solid sample of **4** reached a stable level, but the mass lost by the oily sample of **5** continued to increase with the length of time spent under vacuum due to its liquid state which permits further reaction. These observations are consistent with a shift in the equilibrium upon which the volatile corresponding dichlorosilane is removed under vacuum. In an NMR tube experiment, the microscopic reverse reaction of a 1:1 mixture of **5** and Et_2SiCl_2 produced **11** completely at room temperature.

$$2\ R_2Si(OPO)Cl \rightleftharpoons R_2SiCl_2 + R_2Si(OPO)_2 \quad (5)$$

10 (R = Me) **4** (R = Me)
11 (R = Et) **5** (R = Et)

Attempts to prepare cleanly the mixed chloro derivatives $(CH_2)_3Si(OPO)Cl$ and $Ph_2Si(OPO)Cl$ were unsuccessful. Reaction of $(CH_2)_3SiCl_2$ with 1 equiv. each of HOPO and NEt_3 in THF

produced the disubstituted product, **8**, in 55% isolated yield. However, evidence for the formation of $(CH_2)_3Si(OPO)Cl$ was seen in an NMR tube reaction of $(CH_2)_3Si(OPO)_2$ and $(CH_2)_3SiCl_2$ in 1:1 ratio resulting in a mixture of **8**, $(CH_2)_3SiCl_2$, and $(CH_2)_3Si(OPO)Cl$ in about 1:1:1 ratio by peak height in the ^{13}C NMR spectrum, along with other unidentified species. Attempts to form $Ph_2Si(OPO)Cl$ by transsilylation of Ph_2SiCl_2 with 1 equiv. of **1** led to the formation of **9**, Me_3SiCl, and unreacted Ph_2SiCl_2. An NMR tube experiment of the combination reaction of **9** and Ph_2SiCl_2 in 1:1 ratio in DMSO-d_6 also failed to produce any detectable $Ph_2Si(OPO)Cl$.

Comparative ^{13}C NMR Analysis. A comparison of the ^{13}C NMR spectra of monosubstituted complexes was done to probe the electronic changes that occur within the OPO ligand on chelation (Figure 11). The spectra of **1**, **3**, and **10** in $CDCl_3$ are shown in order of their decreasing Si←OC bond lengths (**1** > **3** > **10**) which have been measured crystallographically (Figure 12). The spectrum of HOPO in $CDCl_3$ is also shown with peak assignments made on the basis of previous assignments.[22] Comparing the spectra of **3** and **10**, carbons **a**, **b**, and **e** are observed to shift upfield and carbons **c** and **d** are observed to shift downfield as the strength of the Si←OC interaction increases. Carbon **a** was much less sensitive to chelation than carbons **b**, **c**, **d**, and **e**, despite its closest proximity to silicon. Smaller shifts of carbon **a** are attributed to competing electronic effects of deshielding caused by Si←OC coordination and shielding caused by delocalization of the nitrogen lone pair into the pyridine ring, in which the delocalization effect wins out for a net small shielding effect. This is in contrast to net deshielding effects observed in acetamide silicon complexes in which π-delocalization should also be possible. In those cases, downfield shifts of the C=O resonance by as much as 7 ppm were observed.[9]

A comparative analysis of ^{13}C NMR spectra of the entire series of $R_2Si(OPO)_2$ derivatives was also done for which all were largely similar (see Supporting Information). All of their peaks appeared in the continuum between the spectra of **3** and **10** as expected based on their comparative Si–O bond lengths. These trends further support ^{13}C NMR spectroscopy as a tool to characterize qualitatively OPO chelate formation and chelation strength as a consequence of π-delocalization.

Figure 11. Delocalization of π electrons upon chelate ring formation

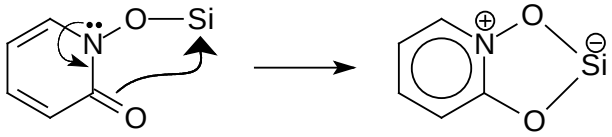

Figure 12. Partial ^{13}C NMR spectra of HOPO and **1**, **3**, and **10** in $CDCl_3$ at room temperature in order of increasing Si←OC bond strength.

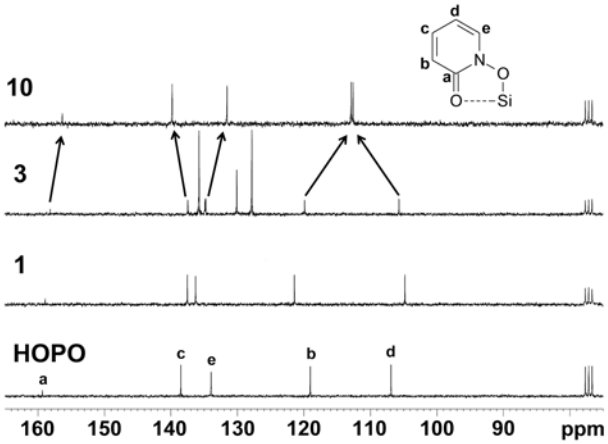

A comparison of the peak locations of the free HOPO ligand and **3** indicates that the influence of the Si←OC interaction in **3** is similar but slightly weaker than the H-bonding interaction(s) that occur in HOPO in solution.[34] This is evidenced by carbon resonances **b** and **d** being closer together and **c** and **e** being farther apart in HOPO than in **3**. One inconsistency is the lower field appearance of carbon **a** of HOPO vs. **3** which is probably due to the larger inductive effect by H vs. Si. The observed effect of H-bonding donor solvents and the crystal structure of **3**·Ph_3SiOH·½C_5H_{12} described later further support the energetic similarity of H-bonding to Si←OC coordination in **3**.

Dynamic Behavior in Monosubstituted OPO Complexes. A VT-NMR study of **3** in toluene-d_8 revealed an upfield shift of its ^{29}Si NMR resonance from –19.4 ppm to –41.0 ppm with decreasing temperature from 60 °C to –95 °C (see Supporting Information).[35] This observation is consistent with a rapid equilibrium between 4- and 5-coordinate states with the

latter favored at lower temperatures (eq 6). The appearance of a single ^{29}Si NMR resonance at all temperatures is consistent with the process occurring at a rate faster than the NMR timescale. A ^{13}C VT-NMR study of **3** showed shifts of all five OPO ligand resonances in the directions consistent with an increased population of its coordinated form with decreasing temperature as discussed in the comparative NMR analysis above (Figure 13). Broadening of all five OPO carbon resonances was observed at approximately –80 °C indicating slowing of the chelation reaction and yielded an activation barrier of ca. 9.9 kcal/mol. The carbonyl resonance remained comparatively sharp which is consistent with its lower sensitivity to changes in chemical shift between coordinated and uncoordinated states.

Figure 13. Plot of the ^{13}C NMR chemical shifts of **3** in toluene-d_8 vs. temperature. Carbon resonances associated with the OPO ligand are indicated with a *.

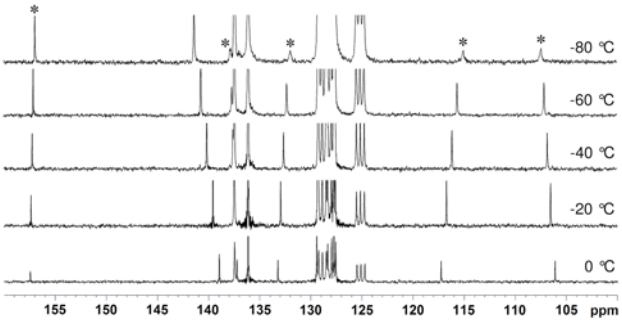

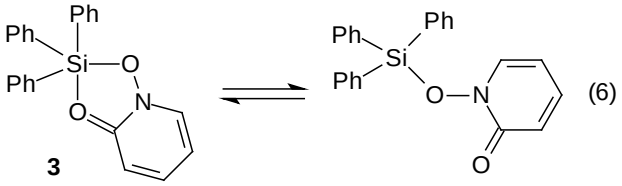

A solvent-dependent ^{29}Si NMR chemical shift for **3** was also observed with its resonance appearing at –22.8 ppm in toluene-d_8, –22.3 ppm in C_6D_6, and –11.5 ppm in $CDCl_3$ at room temperature. The lower field appearance in $CDCl_3$ is attributed to a shift in the equilibrium caused by a non-classical hydrogen-bonding interaction between the solvent and the carbonyl oxygen atom of the ligand. A similar argument has been made for the solvent-dependent chemical shifts in neutral salen-type,[7] hydrazide,[8] and acetamide silicon complexes.[9] On warming **3** from 23 °C to 60 °C in $CDCl_3$, its ^{29}Si NMR resonance was observed to shift

downfield by only 0.7 ppm to −10.8 ppm which suggests that nearly all of the tetracoordinate form is present.

The addition of methanol, a stronger H-bonding donor, resulted in protonolysis of **3** to form HOPO, but the addition of the bulkier Ph_3SiOH proved to be a compatible mixture for an NMR study of the H-bonding interaction (Figure 14).

Figure 14. ^{29}Si NMR spectra (toluene-d_8) of **3**, Ph_3SiOH, and solutions of both in the indicated Ph_3SiOH:**3** mole ratios. The peaks associated with **3** are indicated with a *.

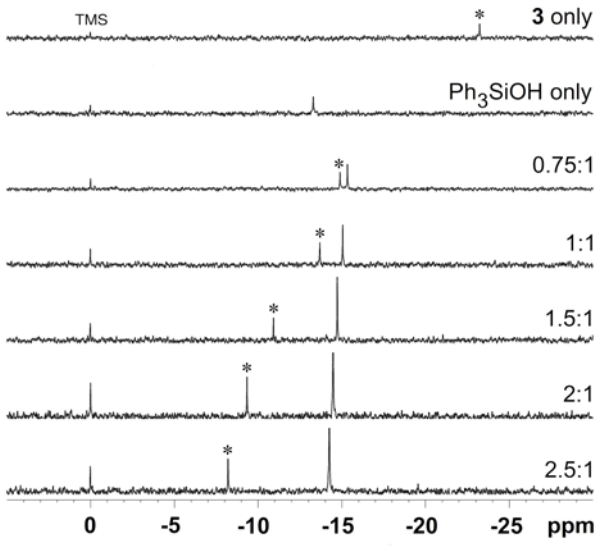

In a 1:1 molar mixture of **3** and Ph_3SiOH in toluene-d_8, the ^{29}Si NMR chemical shift of **3** was shifted 9.5 ppm downfield and the chemical shift of Ph_3SiOH was shifted 1.8 ppm upfield from their native positions at room temperature. These shifts reflect the expected deshielding of the silicon atom in **3** due to elongation of the dative Si←OC bond and a slight shielding of the silicon atom in Ph_3SiOH resulting from an increase in electron density on oxygen. Increasing the concentration of Ph_3SiOH further weakened the chelate as evidenced by further downfield shifts of **3**. These observations are consistent with a fast exchange equilibrium in forming an adduct (eq 7). Heating the solution containing a 1:1 ratio of **3** and Ph_3SiOH from 23 °C to 70 °C resulted in shifting of both peaks toward their native positions but only at a very low rate of <0.01 ppm/°C which reflects only a slight weakening of the H-bonding interaction with temperature and therefore a small enthalpy change between states.

3 + Ph_3SiOH ⇌ **3**·Ph_3SiOH (7)

The solution of Ph_3SiOH:**3** in 2.5:1 ratio was found to be metastable and precipitated a solid immediately following its NMR analysis. A repeated NMR analysis following precipitation suggested the solid to be "**3**·Ph_3SiOH" as evidenced by the disappearance of **3** and a decrease in the intensity of Ph_3SiOH and that no additional peaks were observed. This assignment is supported by the successful isolation of a crystal of this adduct, **3**·Ph_3SiOH·½C_5H_{12},[36] and provides structural evidence for the weakening of the Si←OC interaction by H-bonding donors (Figure 15). The co-crystallized adduct confirms hydrogen-bonding ($d_{H\cdots O}$ = 1.86(4) Å) between Ph_3SiOH and the carbonyl oxygen atom of **3**. In comparison to the pure form of **3**, the C=O distance in **3**·Ph_3SiOH·½C_5H_{12} is shortened by 0.017(4) Å and the dative Si←OC bond is significantly elongated by 1.181(2) Å. The near complete dissociation of the Si←OC bond also results in the expected change in geometry of the $Ph_3Si(OPO)$ molecule from a distorted TBP to a distorted tetrahedral structure [all ∠O–Si–C's and ∠C–Si–C's range from 102.7° to 113.3°]. Given that the Si←OC bond of **3** is nearly fully dissociated in the adduct, the ^{29}Si NMR chemical shift prior to its abrupt precipitation in the NMR study was viewed as a reasonable estimate of the upper temperature limit in the ^{29}Si VT-NMR study. With this value and a lower temperature limit of the chemical shift at –95 °C where **3** precipitates, the equilibrium concentrations of 5- and 4-coordinate modes were calculated at each temperature using their ^{29}Si NMR chemical shifts as weighted averages of the two states.[6a] A plot of ln K_{eq} vs. 1/T afforded thermodynamic values of $\Delta H = +12.8 \pm 0.3$ kJ·mol^{-1} and $\Delta S = +49.3 \pm 1.2$ J·mol^{-1}·K^{-1} for the dissociation reaction (Figure 16).

Figure 15. Crystal structure of **3**·Ph_3SiOH·½C_5H_{12} at the 50% probability level. The pentane molecule is omitted for clarity.

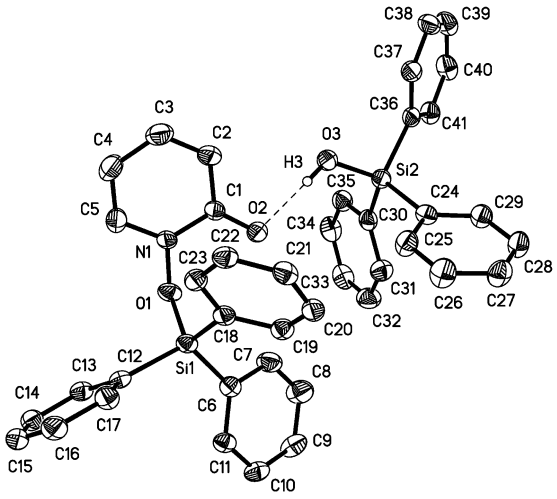

Figure 16. Plot of ln K_{eq} vs. 1/T for the equilibrium between 5- and 4-coordinate states of **3** in toluene-d_8. Linearized equation: ln K_{eq} = 1541.3(1/T) – 5.9315; R^2 = 0.9963.

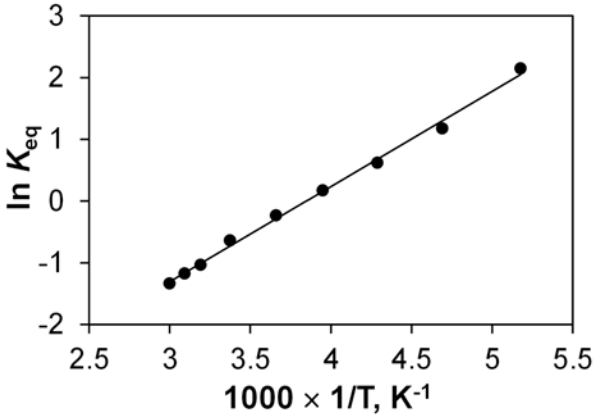

A solvent-dependent ^{29}Si NMR chemical shift was observed for **1** with its resonance appearing at ~6 ppm lower field in $CDCl_3$ than in toluene-d_8, which seemed to suggest a solvent-assisted weakening of the already weak Si←OC interaction observed in its crystal structure. With these observations, a chemical shift dependence on temperature might also be expected in the non-hydrogen bonding solvent, toluene-d_8, but this was not observed (^{29}Si NMR: 30.6 ppm, –90 °C; 29.1 ppm, 50 °C). Furthermore, the direction of the slight shift was opposite that for a dissociative process. It is therefore concluded that the dative Si←OC interaction in **1** is

effectively non-existent in solution because of general entropy effects that promote dissociation and that the lower field ^{29}Si resonance in $CDCl_3$ vs. toluene-d_8 is caused by a hydrogen-bonding donor interaction with the hydroxylamine oxygen leading toward protonolysis of the OPO ligand. A similar subtle effect is likely to exist in all of the other OPO complexes studied here which is not unreasonable in light of the extreme sensitivity of all of these complexes to moisture.

For **10**, only a small solvent dependence of its ^{29}Si NMR chemical shift was observed (–39.5 ppm, toluene-d_8; –38.0 ppm, $CDCl_3$) and a ^{29}Si VT-NMR study in toluene-d_8 showed a continuous downfield shift with increasing temperature at a very low rate of ~0.02 ppm/°C from –80 °C to 24 °C, similar to the small rate of change observed for the $Ph_2Si(OPO)_2$ derivative described below. Although a fast Si←OC bond dissociation is possible, the presence of C–H···Cl contacts would also result in deshielding of the ^{29}Si nucleus.[37] The chelation of OPO in **10** in comparison to **1** is consistent with the greater electron-withdrawing power of chloride vs. methyl. In comparison with the other 5-coordinate OPO complexes, the shorter Si–OC bond distance in **10** vs. **3** and **7** is consistent with its greater coordinative stability in solution.

Dynamic Behavior in Disubstituted OPO Complexes. ^{29}Si VT-NMR studies of **4**, **5**, **6**, **8**, and **9** all showed downfield shifts with increasing temperature which suggests, in each case, a rapid equilibrium between 6- and 5-coordinate states by dissociation of a dative Si←OC bond (eq 8). Taking **4**, **5**, **6**, **8**, and **9** as a whole and with room temperature as a point of reference, ^{29}Si NMR resonances appearing further upfield were less responsive to temperature changes (Figure 17).[38] This phenomenon is attributed to an increase in the Si←OC bond strength that is accompanied with an increase in shielding of the Si atom. A correlation between ^{29}Si NMR chemical shift and Si–O bond length has been observed previously for a series of prolinamide complexes.[10,39] The relative strengths of the Si←OC interaction in solution are therefore indicated in the order ^{i}Pr < Et < Me < $(CH_2)_3$ < Ph. Further support for OPO chelation equilibria is given by (1) small shifts of the ^{13}C NMR resonances in directions consistent with increasing chelation with decreasing temperature for **4**, **6**, **8**, and **9**, (2) a solvent dependence of **6** on the ^{29}Si NMR chemical shift (–105.3 ppm, toluene-d_8; –101.1 ppm, $CDCl_3$) indicating the weakening of the Si←OC bond by

the H-bonding donor solvent, and (3) the structure of the bulkier derivative, **7**, which serves as a possible model for the dissociated form of these complexes. These observations and trends indicate that the increase in ancillary ligand sterics for **4**→**5**→**6**→**7** destabilizes chelation of one of the rings and lowers the barrier to Si←OC bond dissociation. The higher barrier to Si←OC bond dissociation in **8** is suggestive of its greater Lewis acidity that has been reported for other ring-strained silacyclobutanes[31] and in comparison with **4**, the results described here suggest that reduced sterics of the constrained ring may also play a role. The markedly lower sensitivity of the ^{29}Si NMR shift to temperature in **9** is consistent with a prior report in which the increased electron-withdrawing power of a phenyl vs. methyl group has been seen to completely suppress dissociation of dative Si←N bonds.[8b]

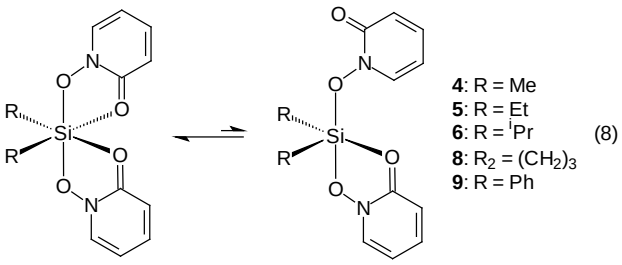

Figure 17. Plot of the ^{29}Si NMR chemical shifts of $R_2Si(OPO)_2$ complexes in $CDCl_3$ vs. their rate of downfield shift with increasing temperature from their native positions at room temperature. For solubility reasons, the rate of change for **9** was recorded in DMSO-d_6.

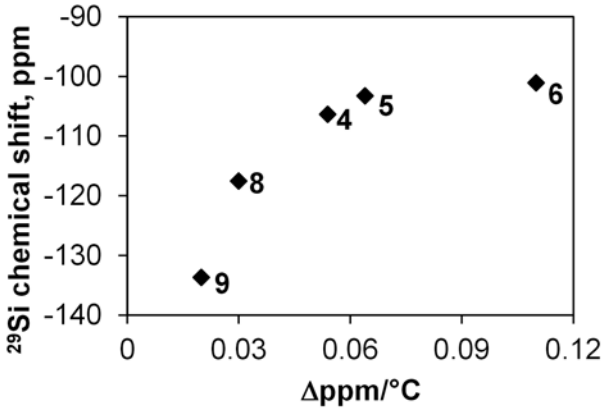

Spectroscopic evidence for the observed diastereomers in the crystal structures of **4**, **6**, **8**, and **9** was obtained by VT-NMR studies. However, due to large differences in solubility between the complexes as well as the influence of the H-bonding donor effects of $CDCl_3$ on the rate of their

interconversion, the choice of solvent was important for their observation. Qualitatively, the solubilities in $CDCl_3$ are **6** > **4** > **8** > **9**, the same order as the Δppm/°C trend, and therefore suggests that looser coordination spheres facilitate dissolution of these $R_2Si(OPO)_2$ complexes. The remarkably similar average Si–O bond lengths in **4**, **5**, and **6** coupled with their measureable differences in coordinative sensitivity to temperature also emphasize the role of solvent in the Si←OC bond dissociation and stereoisomerism equilibria.

^{1}H VT-NMR analysis of **4** was the most informative for the study of the stereodynamic process. On cooling a solution of **4** in toluene-d_8, the initially sharp and magnetically-equivalent methyl group resonance undergoes two simultaneous changes (Figure 18). In one process, a continuous downfield shift of the resonance(s) occurs which is consistent with the gradual increase in methyl deshielding as the extent of Si←OC bond association increases. In the other process, the single methyl resonance broadens and resolves into three equally-spaced (0.057 ppm apart) resonances of unequal intensity in ~20:10:1 ratio. Decoalescence is observed at –65 °C and upon further cooling, the three equally-spaced resonances continue to shift downfield as a group. Taking as an AB site exchange process and using the equation $k = 2\pi\Delta\nu/\sqrt{2}$ affords a first-order rate constant of 62.9 s^{-1} and an activation barrier of ~ 10.3 kcal/mol.[40] The resolved peaks in the lower temperature limit were assigned to the 3 possible diastereomers having O(N)-*trans*-O(N) (**I**), O(N)-*trans*-O(C) (**II**) and O(C)-*trans*-O(C) (**III**) arrangements. By inductive effects, the methyl resonance of **III** would be expected to appear the farthest downfield due to both methyl groups occupying positions *trans* to nitrogen-linked oxygen atoms. Likewise, **I** would be represented farthest upfield having both methyl groups *trans* to carbon-linked oxygen atoms and **II** would exhibit a signal at an average chemical shift between **I** and **III**. Single methyl resonances are expected for the symmetric isomers **I** and **III**, however, that two methyl peaks for the asymmetric **II** are not observed is consistent with the simultaneous fast OPO chelation equilibrium that renders them equivalent on the NMR timescale.

A low temperature ^{1}H NMR study of **6** in toluene-d_8 revealed a similar downfield shift and broadening pattern as in **4** also with an approximate coalescence temperature of –65 °C, but overlapping CH and CH_3 isopropyl resonances obscured the refinement of isomers. The low barrier to exchange in these $R_2Si(OPO)_2$ complexes is in contrast with the absence of evidence to exchange observed in $[Si(OPO)_3]^+$ salts where closely-spaced carbon resonances corresponding

to *fac*/*mer* isomers did not coalesce even with heating to 120 °C and suggests that Si←OC bond dissociation is greatly inhibited by increased attractive forces within the cation.[17]

Figure 18. ^{1}H VT-NMR spectra (toluene-d_8) of the methyl resonances of **4**. Diastereomers **I**, **II**, and **III** are assigned to O(N)-*trans*-O(N), O(N)-*trans*-O(C), and O(C)-*trans*-O(C) arrangements, respectively.

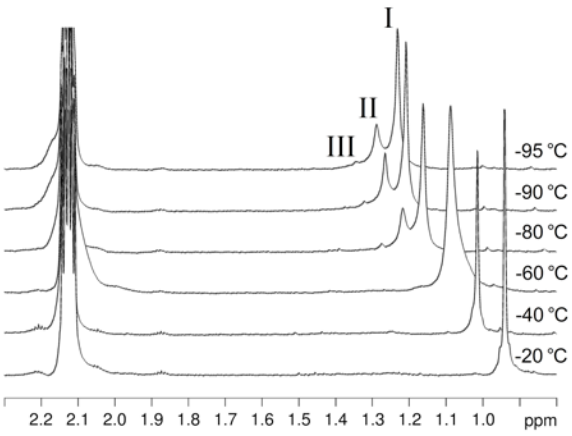

For solubility reasons, a low temperature ^{13}C NMR study of **6** in toluene-d_8 was only barely possible, and not for **8** or **9**. In this study, the two dynamic processes paralleling those observed in the ^{1}H NMR spectra of **4** were observed with the dissociative process evidenced by small shifts of all five OPO carbon resonances in directions consistent with greater coordination at lower temperatures down to –85 °C.[41] The stereoisomerism process was evidenced by pronounced broadening of carbons **c** and **d** only (assignments given in Figure 12), which is distinguished from a purely dissociative process where broadening of all five carbon resonances is observed, as in **3**. A coalescence temperature of about –65 °C was observed and produced new peaks at –80 °C but specific isomers could not be identified unambiguously due to weak signal and overlap with large solvent peaks (see Supporting Information). The rates of isomerization of both **4** and **6** were faster in $CDCl_3$ compared to those in toluene-d_8 as evidenced by significantly less broadening of ^{13}C NMR resonances **c** and **d** at the same temperature of –60 °C (see Supporting Information). The selective broadening of resonances **c** and **d**, representing carbon atoms farthest from the silicon center, is curious. This is due presumably to their greater sensitivity than the other carbons to electronic changes between *N*-oxide and 2-pyridinone tautomeric forms, especially for carbon **d** as reported by Ballesteros, et al.[22]

Compounds **8** and **9** were studied by VT-NMR in $CDCl_3$. In the ^{13}C NMR spectra of both of these complexes, broadening of carbons **c** and **d** is evident at room temperature, with the extent of broadening being greater for **9**. Cooling a solution of **8** to −60 °C resulted in decoalescence and resolution of carbons resonances **a**, **c**, and **d** into two peaks each of unequal intensity all in about 4:1 ratio, and therefore indicates the resolution of only two major isomers (Figure 19). Correspondingly at −60 °C, ^1H NMR doublet resonances at positions **b** and **e** both resolved into two doublets also in about 4:1 ratio while other resonances remained overlapping. A first-order rate constant of 217 s^{-1} was determined for this two-state process affording an activation barrier of ca. 12.5 kcal/mol. Based on the C/N disorder ratios in the crystal of **8** which indicate a relatively lower probability of diastereomer **III**, the two sets of ^1H and ^{13}C NMR resonances, some of which overlap, are assigned to diastereomers **I** and **II**. The larger set of resonances is assigned to **I** and represents two symmetry-equivalent OPO ligands. For the asymmetric **II**, two pairs of doublet resonances corresponding to protons closest to silicon are expected for which only one pair is resolved and the other pair is believed to be coincident with the doublet resonances of **I**. With this assignment, ^1H NMR integration affords a **I**:**II** ratio of 55:45.[42] For **9**, a more complex splitting of carbon resonances was observed on cooling to −60 °C in $CDCl_3$ and suggests perhaps a more even distribution of all three diastereomers (see Supporting Information).

Figure 19. ^{13}C VT-NMR spectra ($CDCl_3$) of the OPO ligand resonances of **8**.

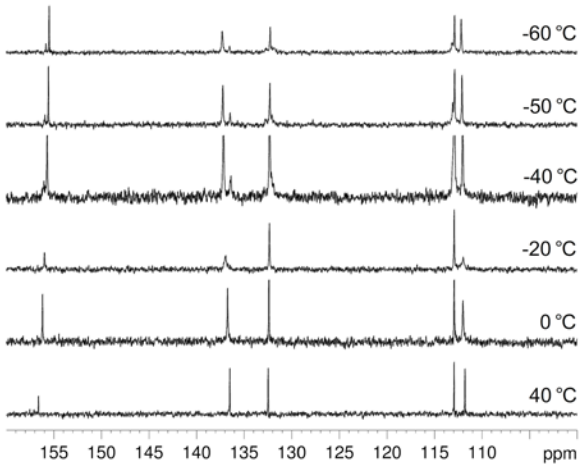

Numerous related stereoisomerism processes in hexacoordinate metal complexes have been described.[43] In many of these prior studies, trigonal (Bailar or Ray and Dutt) twist mechanisms with or without bond rupture have been proposed. Evidence for a bond rupture pathway in this $R_2Si(OPO)_2$ series is given by the fast OPO chelation equilibria at all observable temperatures and the faster isomerization rates of **4** and **6** in the hydrogen-donor solvent $CDCl_3$ vs. toluene-d_8. Furthermore, a comparison of the ^{13}C VT-NMR spectra in $CDCl_3$ indicates a clear trend for the barriers to geometrical isomerization increasing in the order **6** < **4** < **8** < **9** which is the same order as their tendency toward dissociation (Figure 17). Specifically, slightly less broadening of carbons **c** and **d** is observed at –60 °C in **6** compared with **4** at the same temperature, initial broadening is not observed until ~0 °C in **8**, and significant broadening remains even at +60 °C in **9**.

A proposed mechanism for the interconversion of diastereomers in these $R_2Si(OPO)_2$ complexes is given in Figure 20. Although bond rupture processes through square pyramidal (SP) intermediates could be involved in the isomerization process observed here,[44] a mechanism that includes a TBP intermediate with a dangling axial OPO ligand (TBP-axial) is deemed more likely on the basis of the crystal structure of **7** having such an arrangement and on the basis of very few isolated SP neutral silicon complexes.[45] The TBP-axial structure of **7**, represented by **A**, models one of four possible products of Si←OC bond rupture of diastereomer **II**.[46] A reversible Si←^{a}OC bond forming step from **A** leads only to Λ/Δ racemization of **II**. In each of the other TBP intermediates **B**, **C**, and **D**, attack of the dangling ligand in the basal plane gives rise to two possible diastereomers. Intermediates **B** and **C** possess a dangling equatorial OPO ligand (TBP-equatorial) for which Si←OC bond formation may result in reversion back to **II** or on to diastereomers **I** and **III** respectively. Interconversion through TBP-equatorial intermediates **B** and **C** leads to isomerization without inversion whereas interconversion through TBP-axial intermediate **D** results in isomerization simultaneous with inversion. By microscopic reversibility, there cannot be two reversible pathways leading to **III**. Of the two possible intermediates **B** and **D**, intermediate **D** is deemed unlikely due to an increase of 30-40° of ring strain resulting from spanning of the OPO chelate across two eq sites. Thus, inversion can only occur via intermediate **A**.

Figure 20. Proposed mechanism for the interconversion of diastereomers in **4**, **5**, **6**, **8**, and **9**.

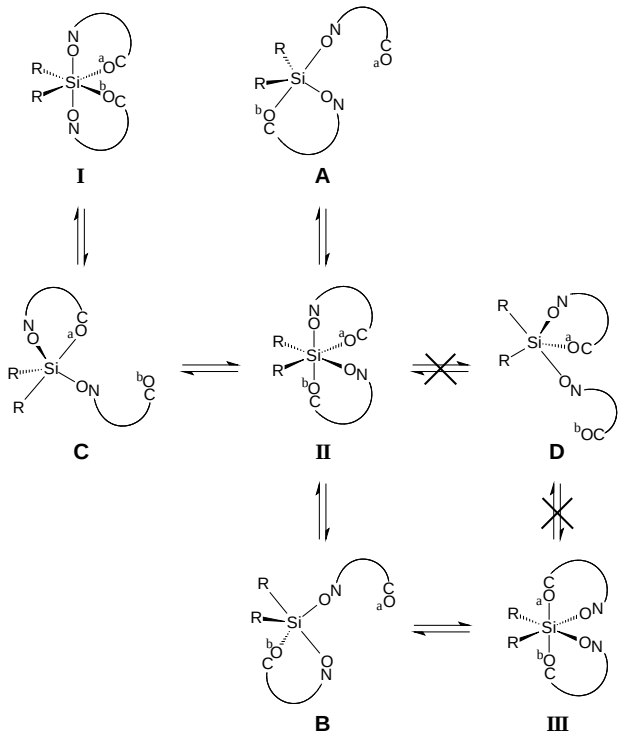

The possibility of recoordination from **A** leading to *trans* alkyl groups was excluded from the mechanism on two bases: (1) To the best of our knowledge, occupancy of alkyl groups in *trans* positions is unprecedented for any neutral 5-coordinate C_2SiX_3 (X = N, O) core, and (2) the same pattern of broadening of OPO carbon resonances in **4**, **6**, and **9** is observed as in the metallacycle **8**, which obviously cannot span both Si–C bonds across two axial sites. With alkyl or Si—ON positions as pivot points, a Berry pseudorotation from **A** followed by Si←OC recoordination leads to either *trans* occupancy of the alkyl groups or to **II** or **III**, and thus does not account for the formation of **I**.

In the proposed TBP intermediates **A** and **C** that lead to the major observed isomers **I** and **II** in **4**, it is noteworthy that their equatorial sites are occupied by groups that form covalent bonds with silicon. This presumably more stable arrangement parallels the bonding-type positional arrangement observed in all of the TBP solid-state structures of **3**, **7**, and **10** as well as in many other TBP silicon chelate complexes.[1,33d] The greater stability of covalently-bound ligands in the equatorial plane has been termed 'equatoriphilicity' which has been invoked in pseudorotation mechanisms in 5-coordinate phosphorus compounds.[47] Also in line with this concept, the higher energy occupancy of one dative Si←OC bond in an equatorial site in the TBP intermediate **B**

leading to **III** is consistent with the far lower abundance of **III** observed in the NMR spectrum of **4**. A similar argument can be made for **5**, **6**, and **8** based on their greater abundance of **I** vs. **III** suggested by their C/N disorder ratios. Accordingly, the more abundant isomer **III** in **9** suggests that intermediate **B** is more accessible than **C**, perhaps due to greater covalent Si–OC bonding in this complex, but this is highly speculative. Although leading to the same products, this mechanism does not account for the possibility of dative Si←ON bond rupture also occurring. Further work is in progress to address this possibility.

Dynamic Behavior in 7. Temperature-dependent ^{29}Si NMR chemical shifts were also observed for the pentacoordinate complex **7** in toluene-d_8 with resonances appearing at higher field with lower temperatures (Figure 21).[48] The extent of shift of the ^{29}Si NMR resonance was smaller than that of **3** which is consistent with its stronger dative Si←OC interaction observed in its crystal structure. All five carbon resonances shifted in directions consistent with greater coordination at lower temperature. As with all other $R_2Si(OPO)_2$ complexes described, these observations are consistent with a fast Si←OC chelation equilibrium, but in this case involving 5- and 4-coordinate states. A large solvent-dependent ^{29}Si NMR chemical shift was observed (toluene-d_8, –62.6 ppm; $CDCl_3$, –54.3 ppm) which again supports the hydrogen-donor assisted Si←OC bond dissociation by the solvent. On cooling to –85 °C in toluene-d_8, the single set of both ^{1}H and ^{13}C NMR OPO ligand resonances became increasingly broadened but did not resolve. From initial line broadening, an activation barrier of ca. 11.5 kcal/mol was determined. The slightly larger barrier to dissociation than in **3** is consistent with the smaller temperature dependence of the ^{29}Si NMR chemical shift. Because of its established 5-coordinate structure and the energetically-accessible 4-coordinate state suggested by the solvent- and temperature-dependent ^{29}Si NMR chemical shift, a hexacoordinate intermediate or transition state would likely be unfavorable energetically. Thus, a purely dissociative mechanism or one involving a bicapped tetrahedral intermediate/transition state[49] is proposed in contrast to an associative process in which one pendant carbonyl group displaces the other. Other degenerate exchange processes in neutral silicon complexes have proposed hexacoordinate intermediates[50] and hexacoordinate transition states.[51]

Figure 21. Plot of the ^{29}Si NMR chemical shift of **7** in toluene-d_8 vs. temperature.

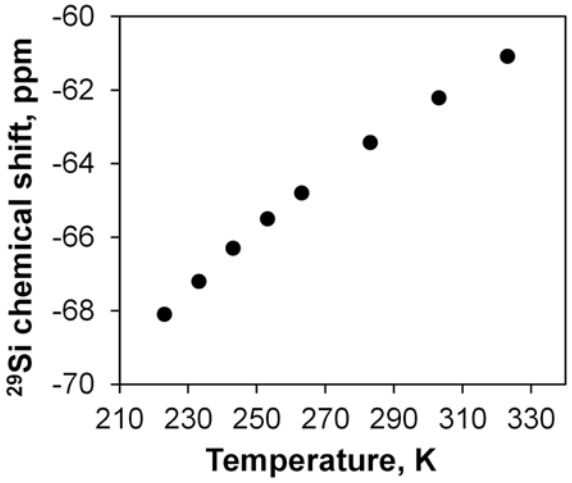

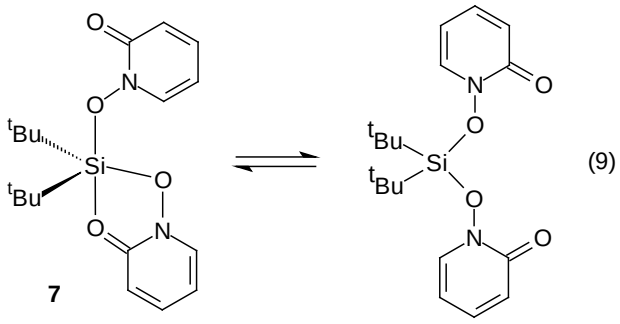

(9)

Conclusion

In the series of organosilicon compounds presented herein, the rigid OPO ligand is coordinatively labile with dissociation occurring through its dative Si←OC bond. Si←OC bond dissociation is facilitated by increasing temperature, increasing core sterics, and by hydrogen-bonding donor interactions. Chelation of the OPO ligand is strengthened by electron-withdrawing ancillary ligands, specifically phenyl and chloride ligands vs. alkyl ligands, as evidenced by structural and VT-NMR comparisons of **1** vs. **3**, **1** vs. **10**, and **4**, **5**, **6**, and **8** vs. **9**. The strength of the OPO chelate is indicated qualitatively by ^{13}C NMR spectroscopy where changes in chemical shift occur as a result of increased π-electron delocalization within the OPO ring.

Experimental Section

All manipulations were performed inside a N_2-filled Vacuum Atmospheres glovebox. Pentane and tetrahydrofuran were dried and vacuum-distilled from purple solutions of benzophenone ketyl and stored over activated 4Å molecular sieves. Acetonitrile, chloroform, and triethylamine were dried and vacuum distilled from activated 4Å molecular sieves. Silyl chlorides were purchased from Gelest, Inc. and used as received. Triphenylsilanol, 1-hydroxy-2-pyridinone (a.k.a. 2-hydroxypyridine *N*-oxide), and DMSO-d_6 were purchased from Aldrich and used as received. ^{1}H, ^{13}C, and ^{29}Si NMR spectra were recorded using a Bruker DPX250 NMR spectrometer (^{1}H, 250.1 MHz; ^{13}C, 62.9 MHz; ^{29}Si, 49.7 MHz) with ^{29}Si NMR spectra recorded at a minimum resolution of 0.36 Hz. ^{29}Si NMR chemical shifts were referenced to external TMS in the same solvent. Infrared spectra were recorded on a Shimadzu Prestige-21 FTIR spectrophotometer. Elemental analyses were performed at the CENTC Elemental Analysis Facility at the University of Rochester.

Crystals were placed onto the tips of glass capillary tubes or fibers and mounted on a Bruker SMART APEX II CCD platform diffractometer for data collection.[52] For each crystal, a preliminary set of cell constants and an orientation matrix were calculated from reflections harvested from three orthogonal wedges of reciprocal space. Full data collections were carried out using MoKα radiation (0.71073 Å, graphite monochromator) with frame times ranging from 10 to 120 seconds and at a detector distance of approximately 4 cm. Randomly oriented regions of reciprocal space were surveyed: four to six major sections of frames were collected with 0.50° steps in ω at four to six different φ settings and a detector position of −38° in 2θ. The intensity data were corrected for absorption.[53] Final cell constants were calculated from the xyz centroids of about 4000 strong reflections from the actual data collections after integration.[54]

Structures were solved using SIR97[55] and refined using SHELXL-2013.[56] Space groups were determined based on systematic absences, intensity statistics, or both. Direct-methods solutions were calculated which provided most non-hydrogen atoms from the E-map. Full-matrix least squares / difference Fourier cycles were performed which located the remaining non-hydrogen atoms. All non-hydrogen atoms were refined with anisotropic displacement parameters. All hydrogen atoms were either placed in ideal positions and refined as riding atoms with relative

isotropic displacement parameters or found from the difference Fourier map and refined freely. Full matrix least squares refinements on F^2 were run to convergence.

In structure **4**, both of the bidentate ligands are modeled as disordered with the planar flips of themselves (66:34 and 79:21, for ligands containing O1/O2 and O3/O4, respectively). The disorder in each bidentate ligand was modeled by refining the sites of the oxygen-linked nitrogen and carbon atoms as a mixture of the two atom types. In each site, the two atom types were constrained to have equivalent positional and anisotropic displacement parameters. For each ligand the sum of the occupancies of the two atom types over those two sites was constrained to be exactly one of each atom type. The same situation occurs for other structures having refined disorder ratios of 81:19 and 82:18 in **5**, 84:16 and 59:41 in **6**, 59:41 and 77:23 in **8**, and 60:40 in **9**. In structure **3**·Ph_3SiOH·½C_5H_{12}, the cocrystallized pentane solvent molecule is modeled as disordered over two general positions (72:28) and over a crystallographic inversion center (50:50). Crystallographic data have been deposited with the Cambridge Crystallographic Data Centre (CCDC). The CCDC numbers are listed in Tables SI1 and SI2.

$Me_3Si(OPO)$ (1). To a stirred solution of 1-hydroxy-2-pyridinone (0.243 g, 2.19 mmol) and NEt_3 (0.32 mL, 2.3 mmol) in THF (14 mL) was added Me_3SiCl (0.28 mL, d = 0.86 g/mL, 2.2 mmol) dropwise at room temperature. The resulting mixture was stirred for 1 day and the NEt_3HCl salt was removed by filtration and washed once with 1 mL of THF. Removal of the solvent under vacuum afforded 0.370 g (92%) of a pale yellow powder. X-ray quality crystals were grown by recrystallization from CH_3CN at –20 °C. ^{1}H NMR ($CDCl_3$): δ 0.32 (s, 9H, CH_3), 6.11 (td, ^3J = 6.9, ^4J = 1.9 Hz, 1H, C*H*CHN), 6.63 (dd, ^3J = 9.2, ^4J = 1.6 Hz, 1H, CHCO), 7.26 (m, 1H, C*H*CHCO), 7.46 (dd, ^3J = 7.1, ^4J = 2.0 Hz, 1H, CHN). ^{13}C NMR ($CDCl_3$): δ 0.3 ((CH_3)$_3$Si), 104.8 (*C*HCHN), 121.4 (*C*HCO), 136.3 (*C*HCHCO or CHN), 137.5 (*C*HCHCO or CHN), 158.9 (CO). ^{29}Si NMR ($CDCl_3$): δ 35.2. FT-IR (KBr, cm^{-1}): 1649(s), 1577(s), 1530(s), 1449(w), 1281(w), 1250(m), 1205(w), 1173(m), 1132(m), 1116(m), 904(m), 851(s), 779(m), 758(m). Anal. Calcd for $C_8H_{13}NO_2Si$: C, 52.43; H, 7.15; N, 7.64. Found: C, 52.49; H, 7.02; N, 7.56.

$Et_3Si(OPO)$ (2). To a stirred solution of 1-hydroxy-2-pyridinone (0.188 g, 1.69 mmol) and NEt_3 (0.25 mL, 1.8 mmol) in THF (14 mL) was added Et_3SiCl (0.28 mL, d = 0.90 g/mL, 1.7 mmol) dropwise at room temperature. The resulting mixture was stirred for 2 days and the NEt_3HCl salt was removed by filtration and washed once with 1 mL of THF. Removal of the solvent under vacuum afforded 0.370 g (98%) of a pale yellow oil. ^{1}H NMR ($CDCl_3$): δ 0.74 (q, 6H, CH_2), 0.92 (t, 9H, CH_3), 6.04 (t, ^3J = 6.8 Hz, 1H, C*H*CHN), 6.53 (d, ^3J = 9.2 Hz, 1H, CHCO), 7.18 (m, 1H, C*H*CHCO), 7.41 (d, ^3J = 7.0 Hz, 1H, CHN). ^{13}C NMR ($CDCl_3$): δ 5.0 (CH_2), 6.4 (CH_3), 104.7 (*C*HCHN), 121.1 (*C*HCO), 136.1 (*C*HCHCO), 137.3 (CHN), 158.8 (CO). ^{29}Si NMR ($CDCl_3$): δ 35.7. FT-IR (KBr, cm^{-1}): 1653(s), 1537(s), 1466(m), 1371(m), 1227(m), 1175(m), 1142(m), 1113(m), 1015(m), 897(m), 845(m), 793(m), 754(s), 596(m). Anal. Calcd for $C_{11}H_{19}NO_2Si$: C, 58.63; H, 8.50; N, 6.22. Found: C, 58.70; H, 8.51; N, 5.93.

$Ph_3Si(OPO)$ (3). To a stirred solution of 1-hydroxy-2-pyridinone (0.150 g, 1.35 mmol) and NEt_3 (0.20 mL, 1.4 mmol) in THF (8 mL) was added a solution of Ph_3SiCl (0.399 g, 1.35 mmol) in THF (2 mL) dropwise at room temperature. The resulting mixture was stirred for 1 hour and the NEt_3HCl salt was removed by filtration and washed once with 1 mL of THF. Removal of the solvent under vacuum afforded a pale yellow solid (0.500 g, 100%). X-ray quality crystals were obtained by recrystallization from THF/pentane by the diffusion method. ^{1}H NMR ($CDCl_3$): δ 5.94 (td, ^3J = 6.9, ^4J = 1.7 Hz, 1H, C*H*CHN), 6.16 (dd, ^3J = 9.1, ^4J = 1.4 Hz, 1H, CHCO), 7.03 (m, 1H, C*H*CHCO), 7.25 (m, 10H, ArH), 7.58 (m, 6H, ArH, CHN). ^{13}C NMR ($CDCl_3$): δ 105.9 (*C*HCHN), 120.1 (*C*HCO), 127.9 (C_6H_5), 130.1 (*p*-C_6H_5), 134.7 (CHN or SiC), 134.9 (CHN or SiC), 135.8 (C_6H_5), 137.5 (*C*HCHCO), 158.3 (CO). ^{29}Si NMR ($CDCl_3$): δ –11.5. FT-IR (KBr, cm^{-1}): 1641(s), 1557(s), 1547(s), 1427(m), 1231(w), 1188(m), 1119(s), 1101(m), 895(w), 754(m), 711(m), 700(m). Anal. Calcd for $C_{23}H_{19}NO_2Si$: C, 74.76; H, 5.18; N, 3.79. Found: C, 74.57; H, 5.23; N, 3.70.

$Me_2Si(OPO)_2$ (4). To a stirred solution of 1-hydroxy-2-pyridinone (0.364 g, 3.30 mmol) and NEt_3 (0.50 mL, 3.6 mmol) in THF (14 mL) was added Me_2SiCl_2 (0.20 mL, d = 1.06 g/mL, 1.7 mmol) dropwise at room temperature. The resulting mixture was stirred for 1 day and the NEt_3HCl salt was removed by filtration and washed once with 2 mL of THF. Removal of the solvent under vacuum afforded 0.385 g (84%) of a pale yellow powder. X-ray quality crystals

were obtained by recrystallization from THF/pentane by the diffusion method. ^{1}H NMR ($CDCl_3$): δ 0.05 (s, 6H, CH_3), 6.60 (m, 2H, C*H*CHN), 6.75 (dd, ^{3}J = 8.7, ^{4}J = 1.4 Hz, 2H, CHCO), 7.39 (m, 2H, C*H*CHCO), 7.94 (dd, ^{3}J = 6.6, ^{4}J = 1.6 Hz, 2H, CHN). ^{13}C NMR ($CDCl_3$): δ 9.4 (CH_3), 111.0 (*C*HCHN), 112.9 (*C*HCO), 132.2 (CHN), 136.4 (*C*HCHCO), 156.3 (CO). ^{29}Si NMR ($CDCl_3$): δ –106.4. FT-IR (KBr, cm^{-1}): 1634(s), 1560(s), 1526(s), 1373(m), 1246(m), 1194(m), 895(w), 797(m), 758(m), 656(m). Anal. Calcd for $C_{12}H_{14}N_2O_4Si$: C, 51.78; H, 5.07; N, 10.06. Found: C, 51.85; H, 4.94; N, 10.05.

$Et_2Si(OPO)_2$ (5). To a stirred solution of 1-hydroxy-2-pyridinone (0.290 g, 2.61 mmol) and NEt_3 (0.38 mL, 2.7 mmol) in THF (14 mL) was added Et_2SiCl_2 (0.20 mL, d = 1.05 g/mL, 1.3 mmol) dropwise at room temperature. The resulting mixture was stirred for 1 day and the NEt_3HCl salt was removed by filtration and washed once with 1 mL of THF. Removal of the solvent under vacuum afforded 0.38 g (95%) of a white powder. X-ray quality crystals were obtained by recrystallization from THF/pentane by the diffusion method. ^{1}H NMR ($CDCl_3$): δ 0.61 (m, 4H, CH_2), 0.86 (m, 6H, CH_3), 6.59 (m, 2H, C*H*CHN), 6.75 (dd, ^{3}J = 8.7, ^{4}J = 1.4 Hz, 2H, CHCO), 7.39 (m, 2H, C*H*CHCO), 7.93 (dd, ^{3}J = 6.6, ^{4}J = 1.6 Hz, 2H, CHN). ^{13}C NMR ($CDCl_3$): δ 10.3 (CH_2), 17.3 (CH_3), 110.8 (*C*HCHN), 112.6 (*C*HCO), 132.2 (CHN), 136.4 (*C*HCHCO), 157.0 (CO). ^{29}Si NMR ($CDCl_3$): δ –103.3. FT-IR (KBr, cm^{-1}): 1632(s), 1560(m), 1534(s), 1378(m), 1365(m), 1248(w), 1192(m), 1018(w), 895(m), 801(m), 757(m), 629(w). Anal. Calcd for $C_{14}H_{18}N_2O_4Si$: C, 54.88; H, 5.92; N, 9.14. Found: C, 54.67; H, 5.79; N, 9.04.

$^{i}Pr_2Si(OPO)_2$ (6). To a stirred solution of 1-hydroxy-2-pyridinone (0.250 g, 2.25 mmol) and NEt_3 (0.35 mL, 2.5 mmol) in THF (14 mL) was added $^{i}Pr_2SiCl_2$ (0.20 mL, d = 1.03 g/mL, 1.1 mmol) dropwise at room temperature. The resulting mixture was stirred for 1 day and the NEt_3HCl salt was removed by filtration and washed once with 1 mL of THF. Removal of the solvent under vacuum afforded 0.35 g (93%) of a pale yellow powder. X-ray quality crystals were obtained by recrystallization from THF/pentane by the diffusion method. ^{1}H NMR ($CDCl_3$): δ 0.97 (m, 14H, C*H*(CH_3)$_2$), 6.56 (m, 2H, C*H*CHN), 6.74 (dd, ^{3}J = 8.7, ^{4}J = 1.4 Hz, 2H, CHCO), 7.38 (m, 2H, C*H*CHCO), 7.91 (dd, ^{3}J = 6.7, ^{4}J = 1.6 Hz, 2H, CHN). ^{13}C NMR ($CDCl_3$): δ 21.0 (CH_3), 23.1 (CH), 110.5 (*C*HCHN), 112.7 (*C*HCO), 132.2 (CHN), 136.3 (*C*HCHCO), 156.7 (CO). ^{29}Si NMR ($CDCl_3$): δ –101.1. FT-IR (KBr, cm^{-1}): 1632(s), 1560(m),

1528(s), 1458(w), 1373(m), 1248(w), 1198(s), 891(m), 806(m), 754(s), 633(m). Anal. Calcd for $C_{16}H_{22}N_2O_4Si$: C, 57.46; H, 6.63; N, 8.38. Found: C, 57.43; H, 6.57; N, 8.21.

^{t}Bu$_2$Si(OPO)$_2$ (7). To a solution of 1-hydroxy-2-pyridinone (0.343 g, 3.09 mmol) and NEt_3 (0.45 mL, 3.2 mmol) in THF (10 mL) was added ^{t}Bu$_2$SiCl$_2$ (0.33 mL, d = 1.01 g/mL, 1.6 mmol) dropwise at room temperature. The resulting mixture was heated to 70 °C for 5 hours and the NEt_3HCl salt was removed by filtration and washed with 2 mL of THF. The solvent was removed under vacuum with mild heating to afford 0.550 g (98%) of viscous pale yellow oil which solidified after several weeks. X-ray quality crystals were obtained by recrystallization from hot pentane/benzene (~20:1). ^{1}H NMR ($CDCl_3$): δ 1.16 (s, 18H, CH_3), 6.34 (td, ^3J = 6.9, ^4J = 1.7 Hz, 2H, C*H*CHN), 6.73 (dd, ^3J = 8.9, ^4J = 1.6 Hz, 2H, CHCO), 7.36 (m, 2H, C*H*CHCO), 7.71 (dd, ^3J = 6.8, ^4J = 1.6 Hz, 2H, CHN). ^{13}C NMR ($CDCl_3$): δ 26.9 (SiC), 29.8 (CH_3), 107.7 (*C*HCHN), 116.5 (*C*HCO), 134.5 (CHN), 137.0 (*C*HCHCO), 158.2 (CO). ^{29}Si NMR ($CDCl_3$): δ –54.3. FT-IR (KBr, cm^{-1}): 1653(s), 1636(s), 1582(m), 1560(m), 1531(s), 1476(m), 1381(m), 1364(w), 1275(w), 1254(w), 1200(m), 1115(w), 899(m), 826(s), 758(s), 646(w), 615(w). Anal. Calcd for $C_{18}H_{26}N_2O_4Si$: C, 59.64; H, 7.23; N, 7.73. Found: C, 59.45; H, 7.21; N, 7.68.

$(CH_2)_3$Si(OPO)$_2$ (8). To a stirred solution of 1-hydroxy-2-pyridinone (0.301 g, 2.71 mmol) and NEt_3 (0.40 mL, 2.9 mmol) in THF (14 mL) was added $(CH_2)_3SiCl_2$ (0.50 mL, d = 1.20 g/mL, 1.4 mmol) dropwise at room temperature. The resulting mixture was stirred for 1 day and the NEt_3HCl salt was removed by filtration and washed once with 1 mL of THF. Removal of the solvent under vacuum afforded 0.37 g (93%) of a white powder. X-ray quality crystals were grown from an undisturbed reaction mixture of 2 equiv. of **1** with $(CH_2)_3SiCl_2$ in CH_3CN. ^{1}H NMR: δ 1.43 (m, 6H, CH_2), 6.71 (m, 2H, C*H*CHN), 6.87 (d, ^3J = 8.5 Hz, 2H, CHCO), 7.48 (m, 2H, C*H*CHCO), 8.00 (d, ^3J = 6.6 Hz, 2H, CHN). ^{13}C NMR: δ 12.0 ($SiCH_2$), 30.9 ($SiCH_2CH_2$), 111.9 (br, *C*HCHN), 112.9 (*C*HCO), 132.4 (CHN), 136.6 (br, *C*HCHCO), 156.4 (CO). ^{29}Si NMR: δ –117.6. FT-IR (KBr, cm^{-1}): 1630(s), 1560(w), 1518(s), 1364(m), 1192(m), 1152(w), 1118(m), 894(m), 809(m), 754(m), 676(m), 653(m), 637(m). Anal. Calcd for $C_{13}H_{14}N_2O_4Si$: C, 53.78; H, 4.86; N, 9.65. Found: C, 53.48; H, 4.99; N, 9.72.

$Ph_2Si(OPO)_2$ (9). To a solution of **1** (0.251 g, 1.37 mmol) in 7 mL of $CHCl_3$ was added a solution of Ph_2SiCl_2 (0.142 mL, d = 1.22 g/mL, 0.685 mmol) in 7 mL of $CHCl_3$ dropwise at room temperature. The mixture was allowed to stand undisturbed for 5 days. Decantation and washing with ~ 1 mL of $CHCl_3$ yielded 0.132 g (48%) of colorless X-ray quality crystals. ^{1}H NMR ($CDCl_3$, 60 °C): δ 6.62 (m, 2H), 6.83 (br m, 2H), 7.11 (m, 6H), 7.40 (m, 2H), 7.63 (dd, ^3J = 7.7, ^4J = 1.5 Hz, 4H), 8.01 (d, ^3J = 5.8 Hz, 2H). ^{13}C NMR ($CDCl_3$, 60 °C): δ 111.7 (br, *C*HCHN), 113.1 (*C*HCO), 126.0 (*p*-C_6H_5), 126.6 (C_6H_5), 132.4 (*C*HCN), 134.7 (C_6H_5), 136.6 (br, *C*HCHCO), 152.0 (SiC), 156.7 (CO). ^{1}H NMR (DMSO-d_6, 80 °C): δ 6.89 (br m), 7.01 (br m), 7.52 (br m), 7.66 (br t), 8.45 (br). ^{13}C NMR (DMSO-d_6, 80 °C): δ 111.8, 112.4, 124.7, 125.6, 132.4, 133.6, 137.3, 152.5, 155.2. ^{29}Si NMR (DMSO-d_6): δ –133.7. FT-IR (KBr, cm^{-1}): 1630(s), 1562(m), 1514(s), 1364(m), 1250(w), 1192(m), 1150(w), 1117(w), 1098(w), 893(w), 810(m), 766(m), 702(m), 685(m), 664(m). Anal. Calcd for $C_{22}H_{18}N_2O_4Si$: C, 65.65; H, 4.51; N, 6.96. Found: C, 65.08; H, 4.51; N, 6.87. In an NMR tube experiment in $CDCl_3$, the same reaction produced Me_3SiCl, **9**, and unidentified impurities which are believed to co-precipitate with **9** although impurities could not be detected in the ^{1}H and ^{13}C NMR spectra of isolated **9** (see Supporting Information). Due to its very low solubility in $CHCl_3$, THF, and CH_3CN, further purification was not possible. Although it was possible to obtain ^{1}H and ^{13}C NMR spectra of **9** in $CDCl_3$ in a transient soluble state, a ^{29}Si NMR peak could not be located due to severe broadening in the slow fluxional regime.

$Me_2Si(OPO)Cl$ (10). To a stirred solution of 1-hydroxy-2-pyridinone (0.275 g, 2.48 mmol) and NEt_3 (0.35 mL, 2.5 mmol) in THF (14 mL) was added Me_2SiCl_2 (0.30 mL, d = 1.06 g/mL, 2.5 mmol) dropwise at room temperature. The resulting mixture was stirred for 30 minutes and the NEt_3HCl salt was removed by filtration and washed once with 1 mL of THF. Removal of the solvent under vacuum at room temperature afforded 0.482 g (96%) of a white powder. X-ray quality crystals were obtained by recrystallization from THF/pentane by the diffusion method. ^{1}H NMR ($CDCl_3$): δ 0.73 (s, 6H, CH_3), 6.86 (m, 1H, C*H*CHN), 6.95 (dd, ^3J = 8.8, ^4J = 1.2 Hz, 1H, CHCO), 7.68 (m, 1H, C*H*CHCO), 8.15 (dd, ^3J = 6.8, ^4J = 1.5 Hz, 1H, CHN). ^{13}C NMR ($CDCl_3$): δ 10.2 (CH_3), 112.6 (*C*HCHN), 112.9 (*C*HCO), 131.6 (CHN), 139.8 (*C*HCHCO), 156.3 (CO). ^{29}Si NMR ($CDCl_3$): δ –38.0. FT-IR (KBr, cm^{-1}): 1634(s), 1564(m), 1526(s), 1373(m), 1260(s), 1182(w), 1115(w), 1030(w), 897(w), 841(m), 800(m), 766(m), 718(w),

627(w). Anal. Calcd for $C_7H_{10}ClNO_2Si$: C, 41.27%; H, 4.95%; N, 6.88%. Found: C, 41.96%; H, 4.99%; N, 7.04% (consistent with ~5% contamination of **4**; see Supporting Information).

$Et_2Si(OPO)Cl$ (11). To a stirred solution of 1-hydroxy-2-pyridinone (0.223 g, 2.01 mmol) and NEt_3 (0.28 mL, 2.0 mmol) in THF (12 mL) was added Et_2SiCl_2 (0.30 mL, d = 1.05 g/mL, 2.0 mmol) dropwise at room temperature. The resulting mixture was stirred for 80 minutes and the NEt_3HCl salt was removed by filtration and washed once with 1 mL of THF. Drying under vacuum at room temperature for 2 hours afforded 0.427 g (92%) of colorless oil. Contamination by **5** was observed in the NMR spectra (see Supporting Information). ^{1}H NMR ($CDCl_3$): δ 1.03 (m, 10H, C*H*$_2$C*H*$_3$), 6.84 (m, 1H, C*H*CHN), 6.97 (dd, ^3J = 8.8, ^4J = 1.2 Hz, 1H, CHCO), 7.68 (m, 1H, C*H*CHCO), 8.15 (dd, ^3J = 6.8, ^4J = 1.5 Hz, 1H, CHN). ^{13}C NMR ($CDCl_3$): δ 7.8 (CH_2), 17.0 (CH_3), 112.4 (*C*HCHN), 112.7 (*C*HCO), 131.6 (CHN), 139.7 (*C*HCHCO), 156.8 (CO). ^{29}Si NMR ($CDCl_3$): δ –35.1.

Supporting Information

Crystallographic tables, CIFs, NMR spectra. This material is available free of charge via the Internet at http://pubs.acs.org.

Author Information

Corresponding Author

* E-mail: bkraft@sjfc.edu

Notes

The authors declare no competing financial interest.

Acknowledgments

The authors thank St. John Fisher College and the University of Rochester Chemistry Department for support, and the many St. John Fisher undergraduates (Matthew Cribbin, Nicole

Gombert, Corinne Kingsley, Christopher Manzella, Arielle Mensch, Drew Merkel, Michelle Putman, Michael Shadeck, Tina Snyder, Seth VanDerVeer, and Rachel Wagner) who contributed to the initial preparation and characterization of many of the compounds, Megan Reesbeck (University of Rochester X-ray Crystallographic Facility) for solving the X-ray structure of **5**, and Dr. Tom Douglas for his assistance with NMR.

References

(1) For reviews, see: (a) Chuit, C.; Corriu, R. J. P.; Reyé, C.; Young, J. C. In *Chemistry of Hypervalent Compounds*; Akiba, K.-Y., Ed.; Wiley-VCH: New York, 1999; p 81. (b) Kira, M.; Zhang, L.-C. *The Chemistry of Hypervalent Compounds*; Akiba, K.-Y., Ed.; Wiley-VCH: Weinheim, Germany, 1999; p 147. (c) Tacke, R.; Pülm, M.; Wagner, B. *Adv. Organomet. Chem.* **1999**, *44*, 221. (d) Holmes, R. R. *Chem. Rev.* **1990**, *90*, 17. (e) Bassindale, A. R.; Glynn, S. J.; Taylor, P. G. In *The Chemistry of Organic Silicon Compounds*; Rappoport, Z.; Apeloig, Y., Eds.; Wiley: Chichester, U.K., 1998; vol. 2, part 1, p 495. (f) Kost, D.; Kalikhman, I. In *The Chemistry of Organic Silicon Compounds*; Rappoport, Z.; Apeloig, Y., Eds.; Wiley: Chichester, U.K., 1998; vol. 2, p 1339. (g) Brook, M. A. *Silicon in Organic Organometallic and Polymer Chemistry*; Wiley: New York, 2000; p 97. (h) Holmes, R. R. *Chem. Rev*. **1996**, *96*, 927. (i) Corriu, R. J. P.; Young, J. C. In *The Chemistry of Organic Silicon Compounds*; Patai, S., Rappoport, Z., Eds.; Wiley: Chichester, U.K., 1989; vol. 1, p 1241. (j) Tacke, R.; Seiler, O. In *Silicon Chemistry: From the Atom to Extended Systems*; Jutzi, P., Schubert, U., Eds.; Wiley-VCH: Weinheim, Germany, 2003; p 324. (k) Chuit, C.; Corriu, R. J. P.; Reye, C.; Young, J. C. *Chem. Rev.* **1993**, *93*, 1371.

(2) Slone, C. S.; Weinberger, D. A.; Mirkin, C. A. *Prog. Inorg. Chem.* **1999**, *48*, 233.

(3) Corriu, R. J. P.; Kpoton, A.; Poirier, M.; Royo, G.; Corey, J. Y. *J. Organomet. Chem.* **1984**, *277*, C25. Corriu, R. J. P. *J. Organomet. Chem.* **1990**, *400*, 81.

(4) (a) Kira, M.; Zhang, L. C.; Kabuto, C.; Sakurai, H. *Chem. Lett.* **1995**, *8*, 659. (b) Azuma, S.; Kojima, M.; Yoshikawa, Y. *Inorg. Chim. Acta* **1998**, *271*, 24. (c) Inoue, T. *Inorg. Chem.* **1983**, *22*, 2435.

(5) Pinnavaia, T. J.; Collins, W. T.; Howe, J. J. *J. Am. Chem. Soc.* **1970**, *92*, 4544.

(6) (a) Brendler, E.; Wächtler, E.; Wagler, J. *Organometallics* **2009**, *28*, 5459. (b) Wagler, J.; Gerlach, D.; Roewer, G. *Chem. Heterocycl. Compd.* **2006**, *42*, 1557. (c) Wada, M.; Suda, T.; Okawara, R. *J. Organomet. Chem.* **1974**, *65*, 335.

(7) (a) Wagler, J.; Böhme, U.; Brendler, E.; Roewer, G. *Organometallics* **2005**, *24*, 1348. (b) Wagler, J.; Brendler, E. *Z. Naturforsch.* **2007**, *62b*, 225.

(8) (a) Gostevskii, B.; Silbert, G.; Adear, K.; Sivaramakrishna, A.; Stalke, D.; Deuerlein, S.; Kocher, N.; Voronkov, M. G.; Kalikhman, I.; Kost, D. *Organometallics* **2005**, *24*, 2913. (b) Kalikhman, I.; Kertsnus-Banchik, E.; Gostevskii, B.; Kocher, N.; Stalke, D.; Kost, D. *Organometallics* **2009**, *28*, 512. (c) Kost, D.; Kalikhman, I. *Acc. Chem. Res.* **2009**, *42*, 303. (d) Kalikhman, I.; Gostevskii, B.; Pestunovich, V.; Kocher, N.; Stalke, D.; Kost, D. *ARKIVOC* **2006**, *5*, 63.

(9) Negrebetsky, V. V.; Negrebetsky, V. V.; Shipov, A. G.; Kramarova, E. P.; Baukov, Yu. I. *J. Organomet. Chem.* **1995**, *496*, 103.

(10) Nikolin, A. A.; Kramarova, E. P.; Shipov, A. G.; Baukov, Yu. I.; Negrebetsky, V. V.; Korlyukov, A. A.; Arkhipov, D. E.; Bowden, A.; Bylikin, S. Y.; Bassindale, A. R.; Taylor, P. G. *Organometallics* **2012**, *31*, 4988.

(11) Sohail, M.; Panisch, R.; Bowden, A.; Bassindale, A. R.; Taylor, P. G.; Korlyukov, A. A.; Arkhipov, D. E.; Male, L.; Callear, S.; Coles, S. J.; Hursthouse, M. B.; Harrington, R. W.; Clegg, W. *Dalton Trans.* **2013**, *42*, 10971.

(12) (a) Tedeschi, C.; Azéma, J.; Gornitzka, H.; Tisnés, P.; Picard, C. *Dalton Trans.* **2003**, 1738. (b) Yraola, F.; Albericio, F.; Corbella, M.; Royo, M. *Inorg. Chim. Acta* **2008**, *361*, 2455. (c) Jacobsen, F. E.; Breece, R. M.; Myers, W. K.; Tierney, D. L.; Cohen, S. M. *Inorg. Chem.* **2006**, *45*, 7306. (d) Xu, L.; Li, Y-Z.; Liu, S-H.; Chen, X-T.; Zhou, J-H. *Acta Cryst.* **2005**, *E61*, m364. (e) Xu, L.; Li, Y-Z.; Chen, X-T.; Ji, X-X. *Acta Cryst.* **2004**, *E60*, m769. (f) Peyroux, E.; Ghattas, W.; Hardré, R.; Giorgi, M.; Faure, B.; Simaan, A. J.; Belle, C.; Réglier, M. *Inorg. Chem.* **2009**, *48*, 10874.

(13) (a) Scarrow, R. C.; Riley, P. E.; Abu-Dari, K.; White, D. L.; Raymond, K. N. *Inorg. Chem.* **1985**, *24*, 954. (b) Gorden, A. E. V.; Xu, J.; Szigethy, G.; Oliver, A.; Shuh, D. K.; Raymond, K. N. *J. Am. Chem. Soc.* **2007**, *129*, 6674. (c) Szigethy, G.; Raymond, K. N. *J. Am. Chem. Soc.* **2011**, *133*, 7942.

(14) (a) Agrawal, A.; de Oliveira, C. A. F.; Cheng, Y.; Jacobsen, J. A.; McCammon, J. A.; Cohen, S. M. *J. Med. Chem.* **2009**, *52*, 1063. (b) Puerta, D. T.; Cohen, S. M. *Inorg. Chem.* **2003**, *42*, 3423. (c) Lewis, J. A.; Tran, B. L.; Puerta, D. T.; Rumberger, E. M.; Hendrickson, D. N.; Cohen, S. M. *Dalton Trans.* **2005**, 2588, and references therein.

(15) Serafím, M. J. S.; Bessler, K. E.; Lemos, S. S.; Sales, M. J. A. *Trans. Met. Chem.* **2007**, *32*, 112.

(16) Weiss, A.; Harvey, D. R. *Angew. Chem.* **1964**, *76*, 818; *Angew. Chem. Int. Ed. Engl.* **1964**, *3*, 698.

(17) Tacke, R.; Willeke, M.; Penka, M. *Z. Anorg. Allg. Chem.* **2001**, *627*, 1236.

(18) Tacke, R.; Burschka, C.; Willeke, M.; Willeke, R. *Eur. J. Inorg. Chem.* **2001**, 1671.

(19) Arkles, B.; Larson, G. L. *Silicon Compounds: Silanes & Silicones*; Gelest Catalog, 2nd ed.

Gelest, Inc., 2008.

(20) For comparison, the ^{29}Si NMR chemical shift of independently-prepared Ph_3SiOPh in $CDCl_3$ was δ –14.6. For the synthesis of Ph_3SiOPh and other spectroscopic data, see Hydrlik, P. F.; Minus, D. K. *J. Organomet. Chem.* **1996**, *521*, 157.

(21) Bondi, A. *J. Phys. Chem.* **1964**, *68*, 441.

(22) Ballesteros, P.; Claramunt, R. M.; Cañada, T.; Foces-Foces, C.; Cano, F. H.; Elguero, J.; Fruchier, A. *J. Chem. Soc. Perkin Trans. 2* **1990**, 1215.

(23) (a) Hartung, J.; Svoboda, I.; Fuess, H.; Duarte, M. T. *Acta Cryst.* **1997**, *C53*, 1629. (b) Wolfe, S.; Hsieh, Y.-H.; Batchelor, R. J.; Einstein, F. W. B; Gay, I. D. *Can. J. Chem.* **2001**, *79*, 1272.

(24) Dinan, F. J.; Tieckelmann, H. *J. Org. Chem.* **1964**, *29*, 1650.

(25) Dilman, A. D.; Levin, V. V.; Korlyukov, A. A.; Belyakov, P. A.; Struchkova, M. I.; Antipin, M. Yu.; Tartakovsky, V. A. *J. Organomet. Chem.* **2008**, *693*, 1005.

(26) James, B. D.; Magee, R. J.; Patalinghug, W. C.; Skelton, B. W.; White, A. H. *J. Organomet. Chem.* **1994**, *467*, 51.

(27) Cella, J. A.; Cargioli, J. D.; Williams, E. A. *J. Organomet. Chem.* **1980**, *186*, 13.

(28) Helmer, B. J.; West, R.; Corriu, R. J. P.; Poirier, M.; Royo, G.; de Saxce, A. *J. Organomet. Chem.* **1983**, *251*, 295.

(29) Xu, C.; Baum, T. H.; Rheingold, A. L. *Inorg. Chem*. **2004**, *43*, 1568.

(30) Due to crystallographic resolution limitations, the affected N and C atoms in each disordered OPO ligand in **4**, **5**, **6**, **8**, and **9** were constrained to have the same coordinates. Thus, the assignments of the C–N, N–O, and C–O bond lengths generated from these coordinates are not well-defined.

(31) Denmark, S. E.; Regens, C. S. *Acc. Chem. Res.* **2008**, *41*, 1486. Spiniello, M.; White, J. M. *Organometallics* **2000**, *19*, 1350.

(32) (a) Kim, K.; Ibers, J. A.; Jung, O.-S.; Sohn, Y. S. *Acta Cryst.* **1987**, *C43*, 2317. (b) Dakternieks, D.; Zhu, H.; Masi, D.; Mealli, C. *Inorg.Chem.* **1992**, *31*, 3601. (c) Li, F.; Li, Y.; Harrison, W. T. A.; Wang, W.; Feng, Y. *Acta Cryst.* **2008**, *E64*, m87. (d) Muthalib, A. F. A.; Baba, I.; Tahir, M. I. M.; Tiekink, E. R. T. *Acta Cryst.* **2011**, *E67*, m386.

(33) (a) Weinmann, M.; Gehrig, A.; Schiemenz, B.; Huttner, G.; Nuber, B.; Rheinwald, G.; Lang, H. *J. Organomet. Chem.* **1998**, *563*, 61. (b) Kalikhman, I.; Gostevskii, B.; Girshberg, O.; Sivaramakrishna, A.; Kocher, N.; Stalke, D.; Kost, D. *J. Organomet. Chem.* **2003**, *686*, 202. (c) Kalikhman, I.; Krivonos, S.; Ellern, A.; Kost, D. *Organometallics* **1996**, *15*, 5073. (d) Corriu, R.

J. P.; Kpoton, A.; Poirier, M.; Royo, G.; de Saxcé, A.; Young, J. C. *J. Organomet. Chem.* **1990**, *395*, 1.

(34) Gardner, J. N.; Katritzky, A. R. *J. Chem. Soc.* **1957**, 4375.

(35) To illustrate the significance of these changes in chemical shift, the ^{29}Si NMR shift of Ph_3SiOPh, incapable of chelation, appeared upfield by 0.04 ppm (in the reverse direction) upon heating from 23 °C to 60 °C in $CDCl_3$.

(36) A crystal of the adduct was obtained by partial hydrolysis of **3** in a recrystallization vial containing THF and pentane.

(37) Brendler, E.; Heine, T.; Hill, A. F.; Wagler, J. *Z. Anorg. Allg. Chem.* **2009**, *635*, 1300.

(38) To illustrate the significance of these changes in chemical shifts, the ^{29}Si NMR shift of $Me_2Si(OPh)_2$, incapable of chelation, appeared upfield by 0.44 ppm (in the reverse direction) upon heating from 23 °C to 60 °C in $CDCl_3$, for a rate of change of –0.012 ppm/°C.

(39) A correlation of ^{29}Si NMR chemical shifts with Si–OC bond length could not be made in this series of complexes due to C/N disorder in the crystal structures.

(40) Green, M. L. H.; Wong, L.-L.; Sella, A. *Organometallics* **1992**, *11*, 2660.

(41) Because of a very weak signal resulting from low solubility in toluene-d_8, ^{13}C NMR spectra of **4** were obtainable only to –60 °C.

(42) This result is not wholly consistent with the C/N disorder ratios measured in the crystal structure (indicating a maximum of 36% **I** when constrained to include isomers **I** and **II** only). However, it should be considered that one isolated crystal may not represent the bulk solution or solid sample.

(43) For general kinetics and mechanisms of stereoisomerism in 6-coordinate chelate complexes, see Serpone, N.; Bickley, D. G. *Prog. Inorg. Chem.* **1972**, *17*, 391. For $M(OPO)_3$ [M = Co, Fe], see ref 13a; for tropolonato complexes, see ref 4; for acac-type complexes, see refs 5, 29, and Gordon, II, J. G.; Holm, R. H. *J. Am. Chem. Soc.* **1970**, *92*, 5319.

(44) Eaton, S. S.; Hutchison, J. R.; Holm, R. H.; Muetterties, E. L. *J. Am. Chem. Soc.* **1972**, *94*, 6411.

(45) For $Si(O_2C_6H_4)_2\{OP(NC_5H_{10})_3\}\cdot CH_2Cl_2$, having nearly a SP geometry strongly influenced by hydrogen-bonding of the solvent, see Hey-Hawkins, E.; Dettlaff-Weglikowska, U.; Thiery, D.; Von Schnering, H. G. *Polyhedron* **1992**, *11*, 1789.

(46) For simplicity, only the TBP forms are shown in Figure 20 and not the initial species (a canonical SP arrangement) formed upon vacating an octahedral coordination site. For these representations, see Gordon, II and Holm in ref 39. The TBP intermediates are formed by movement of one of the four possible basal positions of the SP into the basal plane of the newly formed TBP.

(47) Wasada, H.; Hirao, K. *J. Am. Chem. Soc.* **1992**, *114*, 16.

(48) Precipitation ensued at lower temperatures.

(49) Kost, D.; Kalikhman, I.; Krivonos, S.; Stalke, D.; Kottke, T. *J. Am. Chem. Soc.* **1998**, *120*, 4209.

(50) Handwerker, H.; Leis, C.; Probst, R.; Bissinger, P.; Grohmann, A.; Kiprof, P.; Herdtweck, E.; Blümel, J.; Auner, N.; Zybill, C. *Organometallics* **1993**, *12*, 2162.

(51) Belzner, J.; Schär, D.; Herbst-Irmer, R.; Kneisel, B. O.; Noltemeyer, M. *Tetrahedron* **1998**, *54*, 8481.

(52) *APEX2*, version 2010.7-0; Bruker AXS: Madison, WI, 2010.

(53) Sheldrick, G. M. *SADABS*, version 2008/1; University of Göttingen: Göttingen, Germany, 2008.

(54) *SAINT*, version 7.06A; Bruker AXS: Madison, WI, 2003.

(55) Altomare, A.; Burla, M. C.; Camalli, M.; Cascarano, G. L.; Giacovazzo, C.; Guagliardi, A.; Moliterni, A. G. G.; Polidori, G.; Spagna, R. *SIR97: A new program for solving and refining crystal structures*; Istituto di Cristallografia, CNR: Bari, Italy, 1999.

(56) Sheldrick, G. M. *SHELXL-2013/4*; University of Göttingen: Göttingen, Germany, 2013.